



A seismic stratigraphic analysis of Mariana forearc basin evolution

Emily Chapp, Brian Taylor, Adrienne Oakley, and Gregory F. Moore

SOEST, University of Hawaii, Honolulu, Hawaii 96815, USA (chapp@soest.hawaii.edu)

[1] New seismic data collected in the 14.5°–18.5°N Mariana segment of the Izu-Bonin-Mariana island arc system image six seismic stratigraphic sequences that can be mapped throughout the inner forearc. These sediments were most likely deposited from 35 Ma to the present. The oldest stratigraphic Units 1, 2, and 3 are syn-rift volcanoclastic deposits. Unit 4 deposits accumulated during a period of mild structural inversion, which resulted in several isolated reverse-faulted anticlines within the forearc sedimentary basin. A late period of extensional deformation began near the end of Unit 5 deposition and continued through Unit 6 sedimentation to the present. Seismic lines show that the basement of the forearc is composed of large rotated fault blocks and half grabens with NE, NW, and NNE trends. Fault offset calculations show that basement faults with dips between 45° and 50° account for only ~4% total extension in the forearc. South of 16.3°N, normal growth faults initiated during basement extension offset the frontal arc high from a deep forearc basin. From correlations with the known geologic history, we hypothesize that extension during deposition of Units 1 through 3 corresponds to rifting of the Eo-Oligocene Arc, between ~35 Ma and 29 Ma, older deposits being too thin to be seismically resolvable. Localized compression during Unit 4 accumulation occurred some time after Eo-Oligocene rifting in the early Miocene. Late-stage normal faulting near the end of deposition of Unit 5 and throughout Unit 6 accumulation may be associated with the opening of the Mariana Trough backarc basin from ~8 Ma years to the present. There is a higher density of these later faults in the inner forearc between 15.5° and 17°N and in the outer forearc between 14°N and 18°N. Recent extension is at least partially accommodated by reactivation of older basement faults with the same NE, NW, and NNE- trends. Stratigraphic relationships indicate that the inner forearc south of 16.3°N has differentially subsided and tilted trenchward, possibly as a result of a recent change in subducting slab geometry or subducted relief under the forearc.

Components: 14,414 words, 13 figures, 2 tables.

Keywords: Mariana subduction zone; forearc basin; seismic stratigraphy.

Index Terms: 3060 Marine Geology and Geophysics: Subduction zone processes (1031, 3613, 8170, 8413); 3022 Marine Geology and Geophysics: Marine sediments: processes and transport.

Received 21 February 2008; **Revised** 19 May 2008; **Accepted** 15 July 2008; **Published** 21 October 2008.

Chapp, E., B. Taylor, A. Oakley, and G. F. Moore (2008), A seismic stratigraphic analysis of Mariana forearc basin evolution, *Geochem. Geophys. Geosyst.*, 9, Q10X02, doi:10.1029/2008GC001998.

Theme: Izu-Bonin-Mariana Subduction System: A Comprehensive Overview

Guest Editors: Shuichi Kodaira, Sara Pozgay, and Jeffrey Ryan

1. Introduction

[2] Studies of arc-trench systems have identified the Mariana subduction system as one end-member of the convergent margins on Earth [Forsyth and Uyeda, 1975; Uyeda, 1982; Froidevaux et al., 1988]. It is characterized by subduction of old (lower Cretaceous), thinly sedimented (typically less than 500 m), cold Pacific plate lithosphere [LaTraille and Hussong, 1980; Hussong and Fryer, 1981; Nakanishi et al., 1992], which approaches a near-vertical slab dip beneath the central volcanic arc [Katsumata and Sykes, 1969; Isacks and Barazangi, 1977; Chiu et al., 1991; Engdahl et al., 1998; Stern et al., 2003]. The Mariana system is unique from other convergent margins as the oldest oceanic crust subducts beneath the Philippine Sea plate. System components include a backarc basin that opened by seafloor spreading [Karig, 1971a; Hussong and Fryer, 1983; Hussong and Sinton, 1983; Froidevaux et al., 1988; Martinez et al., 1995, 2000] and active serpentinite seamounts protruding through the outer forearc [Fryer, 1992a, 1992b; Fryer et al., 1999]. This margin lacks great earthquakes common in other subduction zones [Forsyth and Uyeda, 1975; Froidevaux et al., 1988; Huang and Okal, 1998; Hyndman and Peacock, 2003]. The outer forearc does not have a substantial sedimentary cover or accretionary prism [Hussong and Uyeda, 1981; Mrozowski et al., 1981; Bloomer, 1983]. Samples from seafloor drill holes, dredges, and island outcrops reveal three periods of major arc volcanism and growth in the Eo-Oligocene, Mio-Pliocene, and Quaternary [Taylor, 1992]. This volcanic construction was overlapped by three periods of arc rifting and backarc spreading (Eocene, Oligo-Miocene, Plio-Quaternary) since Mariana subduction began ~50 Ma [Taylor, 1992; Cosca et al., 1998].

[3] Surprisingly, the evolution of the forearc basin within this textbook example of an intraoceanic arc-trench system has received comparatively little attention. Where subduction erosion is said to occur, gravitational collapse of the forearc from undercutting of the overlying plate results in a subsided forearc basin [Clift and Vannucchi, 2004; Laursen et al., 2002]. Seismic profiles from the Mariana forearc show that the subducting plate is >25 km below the forearc basin and would most likely not affect the basin [Oakley et al., 2008]. Without a large accretionary prism behind which to dam volcanoclastic sediment, the formation of the Mariana forearc basin is not well understood [Karig, 1971a]. Other proposed mechanisms in-

clude trenchward damming by accreted slices of oceanic crust or rifting and subsidence of the forearc basement [Karig and Ranken, 1983]. Seafloor sampling has found no evidence of the former in the Mariana subduction zone, whereas seismic reflection and drilling studies of the Izu-Bonin system along strike to the north have confirmed the latter [Taylor, 1992]. The question remains whether the Mariana forearc basin has a similar rifting and subsidence origin.

[4] Understanding the evolution of forearc deposition and basement structure is important because it can provide information on past deformation and volcanism of the arc-trench system [Dickinson and Seely, 1979]. The isolation of the Mariana intraoceanic island arc system from any terrigenous input results in an undiluted stratigraphic record of volcanic activity, and its modest sediment cover offers a chance to image basement structure that might otherwise be obscured [Stern and Smoot, 1998].

[5] Multichannel seismic reflection (MCS) data across the Mariana forearc collected in 2002 aboard the R/V *Maurice Ewing* image for the first time the complete sedimentary section and basement structure of the forearc basin from 14°N to 18°N. This data set allows us to reconstruct the evolution of the forearc basin by mapping the seismic stratigraphy, quantifying fault geometries in the inner forearc, and identifying changes in basin structure from north to south. We correlate the six major seismic stratigraphic sequences with likely volcano-tectonic periods and use the sequence boundaries to date the formation of the forearc basin (Eocene to early Oligocene) and subsequent tectonic events. Seismic lines reveal an orthogonal NE- and NW-trending fault set as well as a NNE-trending fault system that offset the seafloor and create large structural blocks throughout the forearc. These were initiated during the late Eocene/early Oligocene rifting event and subsequently reactivated. The seismic data also provides the first evidence for local structural inversion and reverse faulting in the Mariana forearc.

2. Geologic Setting and Previous Work

[6] Subduction beneath the Philippine Sea Plate formed the intraoceanic Izu-Bonin-Mariana island arc system. In the Mariana segment, this subduction system includes an opening backarc basin, active volcanic arc, frontal arc high, forearc basin, and outer-arc high (Figure 1) [Karig, 1971b; Hussong

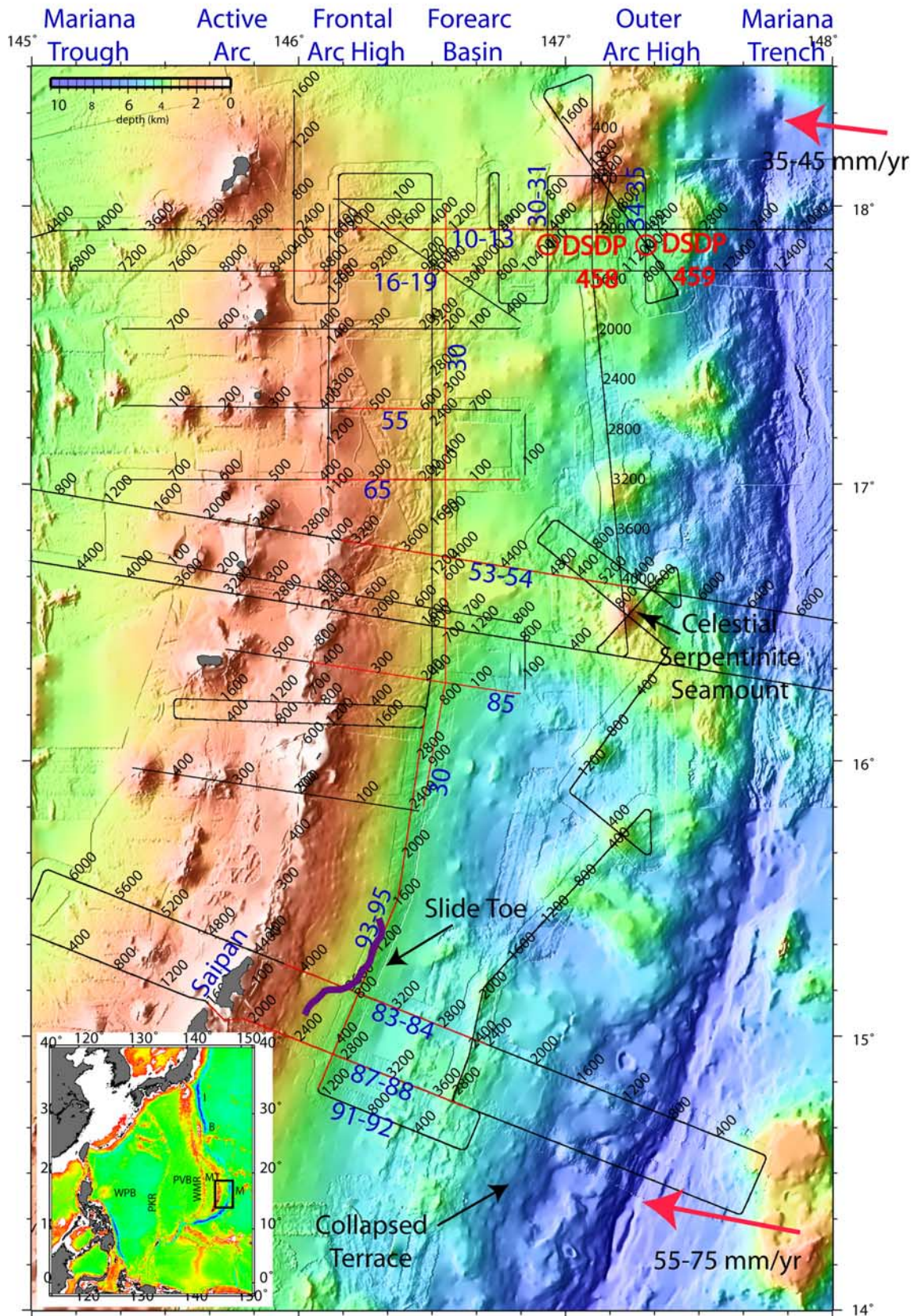


Figure 1

and Uyeda, 1981; Mrozowski *et al.*, 1981; Fryer, 1992b]. The Mariana arc is isolated in the western Pacific Ocean from continental influence and lacks an accretionary prism common to many subduction zones [Hussong and Uyeda, 1981; Mrozowski *et al.*, 1981; Bloomer, 1983].

[7] The structure of the forearc and surrounding island arc system is the result of a complex tectonic history that began with subduction initiation ~ 50 Ma [Taylor, 1992]. The rotation and opening of the West Philippine Basin was contemporaneous with subduction initiation and early volcanism [Sdrolias *et al.*, 2004; Taylor and Goodliffe, 2004]. Counterclockwise rotation of the West Philippine Basin spreading direction to a north-south orientation resulted in massive along-strike stretching of the early Mariana subduction zone. Initial suprasubduction zone volcanism (~ 49 Ma) took the form of extensive seafloor eruptions of boninite and tholeiite lavas creating the igneous basement of the forearc [Cosca *et al.*, 1998; Ishizuka *et al.*, 2006]. A volcanic island arc formed in the Eocene at the location of the present-day frontal arc high. The Eocene arc rifted in the late Eocene to early Oligocene prior to seafloor spreading in the Parece Vela backarc basin, which separated the frontal arc high (Guam to Saipan) from the Palau-Kyushu Ridge remnant arc. DSDP drill cores show that explosive Oligocene volcanism on the frontal arc high continued during rifting until ~ 29 – 31 Ma [Shipboard Scientific Party, 1978a, 1978b; Scott *et al.*, 1980]. This rifting and subsequent spreading, from 29 Ma to 15 Ma, propagated north and south creating the characteristic bow shape of the Mariana subduction zone [Mrozowski and Hayes, 1979; Taylor, 1992; Okino *et al.*, 1998].

[8] Early Miocene volcanism may have slowed or ceased until ~ 20 Ma when the Mio-Pliocene volcanic arc built up slightly west of the rifted Eo-Oligocene arc. DSDP drilling in the Mariana forearc shows an increase in volcanism until 9 Ma [Shipboard Scientific Party, 1978c; 1978d]. The Mio-Pliocene arc was then rifted, and seafloor spreading in the Mariana Trough backarc basin, since ~ 8 Ma, separated the West Mariana Ridge

remnant arc [Seama and Fujiwara, 1993]. This rifting propagated north, further increasing the curvature of the Mariana island arc system.

[9] A third period of explosive volcanism is occurring today throughout the present Mariana Arc, which is building along the rifted Mio-Pliocene arc [Hilton *et al.*, 2005]. GPS studies show the Mariana Trough is continuing to open today and that the forearc is being deformed [Kato *et al.*, 2003; Kitada *et al.*, 2006].

[10] A forearc basin with a width of 50–80 km lies within the inner forearc, bound to the west by the frontal arc high and to the east by the outer arc high. Seismic lines collected prior to and as part of the DSDP Leg 60 drilling project imaged thick sedimentary fill at 18°N (up to 2 s two-way travel time) from $\sim 146.25^\circ\text{E}$ to 147°E . Faulted basement blocks covered by a relatively thin sediment layer, only a few tens to hundreds of meters thick, make up the outer forearc [Mrozowski and Hayes, 1980; Mrozowski *et al.*, 1981]. A discontinuous line of serpentinite seamounts is located on the outer arc high approximately 50–120 km from the trench axis [Fryer, 1992a; Oakley *et al.*, 2006].

[11] DSDP Leg 60 drill sites 458 and 459 are located in the outer forearc region just east of the forearc sedimentary basin in an area of thinly sedimented basement blocks [Mrozowski and Hayes, 1980]. Drill core results show the sediment cover consists of volcanoclastic deposits from Pleistocene to Eocene in age (0.9 Ma to 45 Ma), with the Eocene section <20 m thick [Shipboard Scientific Party, 1978b; Cosca *et al.*, 1998]. Several sedimentary hiatuses are recorded at the drill sites, but two are observed on both drill sites from ~ 3 to 7 Ma and ~ 13 to 14 Ma, possibly representing depositional hiatuses across the basin. Cores recovered at both drill sites sample forearc basement composed of fractured and altered arc tholeiite and boninite eruptions in the form of pillow lavas and massive lava flows. Both drill cores also show normal faulting of sediment and basaltic basement [Shipboard Scientific Party, 1978c, 1978d]. The oldest basement rock recovered was

Figure 1. Shaded bathymetric map of the central Mariana island arc and trench. Black lines indicate the location of all seismic lines and red lines indicate data shown for this manuscript. Red circles show locations for labeled Deep Sea Drilling Program drill sites. Line numbers are annotated in blue and shot numbers are annotated in black. Red arrows show the direction and magnitude of convergence across the forearc. Purple line locates the toe of a submarine landslide. The inset shows a regional map with the survey area denoted by the black box. Labels are as follows: WPB, West Philippine Basin; PKR, Palau-Kyushu Ridge; PVB, Parece-Vela Basin; WMR, West Mariana Ridge; MT, Mariana Trough; IBM, Izu-Bonin-Mariana segments.

49 Ma middle Eocene basalt, supporting the hypothesis that the Mariana forearc basement was created during the initiation of subduction in the Eocene [Shipboard Scientific Party, 1978c, 1978d; Hussong, 1981; Hussong and Uyeda, 1981; Taylor, 1992; Bloomer et al., 1995; Cosca et al., 1998].

[12] Seismic lines collected prior to DSDP Leg 60 drilling of the 18°N transect imaged numerous high angle normal faults that offset both the sediment and basement of the forearc basin [Mrozowski and Hayes, 1980]. Mrozowski and Hayes [1980] suggested that the complex faulting has been continuous since the forearc was formed. Wessel et al. [1994] showed forearc extension occurring at 22°N, accommodated by orthorhombic normal fault sets with a principal NE strike of 44°. They proposed that the fault patterns were a result of radial extension of the forearc due to increased arc curvature associated with back-arc spreading. A less understood orthogonal NE- and NW-trending fault system in the region of 18°N is observed in the forearc [Hussong and Uyeda, 1981; Stern and Smoot, 1998]. The similar NE and NW strikes at 18°N and 22°N suggest that radial extension alone cannot explain these fault trends.

[13] The well-studied Izu-Bonin arc-trench system to the north of the Mariana subduction zone was subject to similar tectonic events making it an obvious analog to the Mariana subduction system. ODP Legs 125 and 126 included several drill holes in the Izu-Bonin forearc region (Sites 782 to 787, 792, and 793) sited on a multichannel seismic survey across the forearc basin. The results show a middle Eocene-age basement in the outer forearc composed of tholeiite and boninite from early volcanism (49–44 Ma) [Taylor, 1992; Cosca et al., 1998; Ishizuka et al., 2006]. The forearc basin formed as a result of an arc rifting event in the early Oligocene which created an irregularly faulted basement of rotated blocks and ridges and preceded back-arc spreading in the Shikoku Basin [Dobson and O'Neil, 1987; Taylor et al., 1990; Taylor, 1992]. The sedimentary fill in the basin is composed of thick volcanoclastic sediment that ranges in age from Oligocene (~31 Ma) to present and is cut by many submarine canyons. Numerous high angle normal faults offset early sediments and basement, similar to what is observed in the Mariana forearc; however, younger sediment in the Izu-Bonin segment does not appear to be faulted like that of the Mariana forearc basin. With similarities in early forearc structure between the

Izu-Bonin and Mariana systems, the question arises as to whether the Mariana forearc basin has a similar arc-rifting origin.

3. Seismic Interpretation

[14] The seismic lines collected over the Mariana forearc basin extend from ~14.5°N to 18.5°N (Figure 1). This area of the forearc can be divided latitudinally into four regions based on bathymetric features. The region from 14°N to 15°N has a narrow inner forearc with a thick sedimentary basin fill, a thinly sedimented midforearc containing rotated blocks making up a series of NNE-, NE-, and NW-trending ridges, and a deep outer forearc with a terrace of presumed serpentinite. This lower slope terrace is not present further north in the Mariana segment but has direct analogs in the Izu-Bonin segment of the IBM system. The frontal arc high bounding the forearc to the west is most pronounced in this region and includes the islands of Rota, Tinian, and Saipan.

[15] From 15.3°N to 16.2°N, the forearc basin widens and deepens, and serpentinite seamounts protrude through the outer forearc high. The seismic lines for this survey do not fully extend across the entire basin here; therefore we are not able to discuss forearc basin structure and stratigraphy for this region. A large bathymetric ridge trends NW across the forearc between 16° and 17°N. The seafloor of the inner forearc is offset by numerous normal faults and the outer forearc contains Celestial Seamount, an active serpentinite mud volcano.

[16] The region between 17°N and 18.5°N has the most irregular seafloor, with numerous fault offsets of both the inner and outer forearc. Several bathymetric highs trend NE and NW across this section of the forearc with Big Blue serpentinite seamount located on the northern edge of the region. The frontal arc high appears diminished or absent in the northernmost survey area. Seismic interpretations for the forearc will be discussed from south to north, in terms of six seismic stratigraphic sequences that can be identified across these regions. Two N-S seismic lines were used to correlate these six units across the survey region. While we were diligent in analyzing the data to tie the events across seismic lines, there is uncertainty when mapping units across such a large region. Although sedimentary deposits exist west of the frontal arc high, this paper will focus on the forearc basin sedimentation.

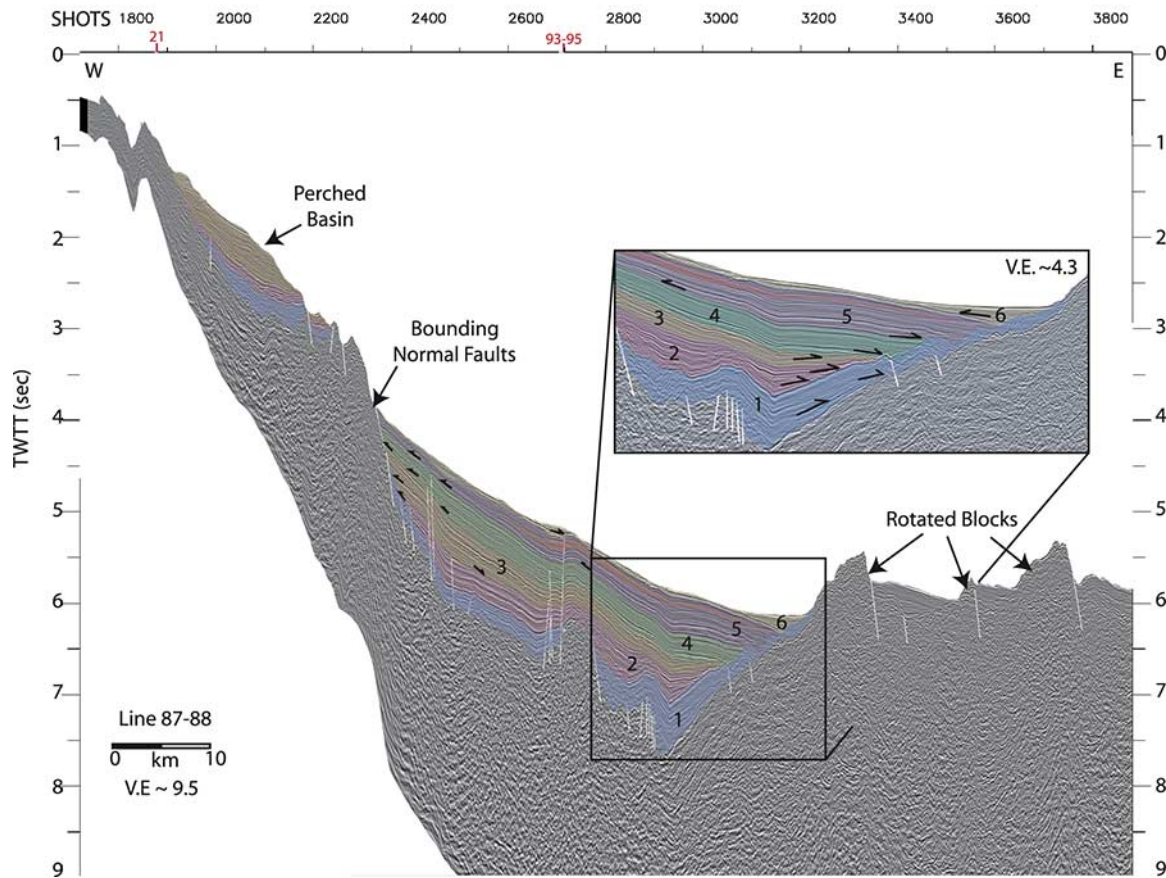


Figure 2. A time-migrated seismic profile of Line 87–88 shows the geometry of the forearc in the 15°N region. Sedimentary units are numbered, and black arrows indicate onlap. The inset shows a blowup of the stratal relations for the eastern side of the basin, at less vertical exaggeration. Local inversion of basement normal faults occurred midway through deposition of Unit 2. Faults are indicated by white lines and seismic data below the seafloor multiple has been cut out. Tie lines are labeled in red on the shot number axis.

3.1. The 15°N Region

[17] The seismic survey of the forearc basin at 14.5°–15°N includes three trench-perpendicular lines and one NNE tie line (Figure 1). Line 87–88 (Figure 2) shows a complete record of the six seismic stratigraphic sequences mapped across the forearc and illustrates the basic geometry of the basin in the southern portion of the survey region. The seismic data show that the southern forearc contains a sedimentary basin, bound on either side by structural highs. On the arcward edge of the basin, a series of normal faults offset the flank of the bounding frontal arc high, separating the main sedimentary basin from a smaller, shallower perched sequence of sediments. The eastern edge of the basin is bound by several rotated basement blocks, resulting from large offset, trenchward dipping (~40°) normal faults. The irregular igneous basement across the southern forearc between

14°N and 15°N is composed of faulted blocks, with fault dips of 40°–45°.

[18] The oldest stratigraphic sequence in the forearc basin is Unit 1 (blue). On the eastern side of the basin, this unit consists of a lower sediment wedge thickening toward the arc that is bedded subparallel to and onlaps the top of the rotated bounding block from SP2910 to SP3050 on Line 87–88 (Figure 2). The wedge shape and basement onlap lead us to interpret Unit 1 as syn-rift sediment deposited during the rifting, which offset and tilted the basement blocks. Thin, uncorrelated sedimentary sequences occur in half graben between rotated basement blocks further east. Unit 1 appears to be folded near SP2900 indicating that a compressional event occurred in the southern forearc after deposition of this unit. On the western side of the basin, Unit 1 makes up a sequence of westward thinning, layered sediment. This deposit is offset on the

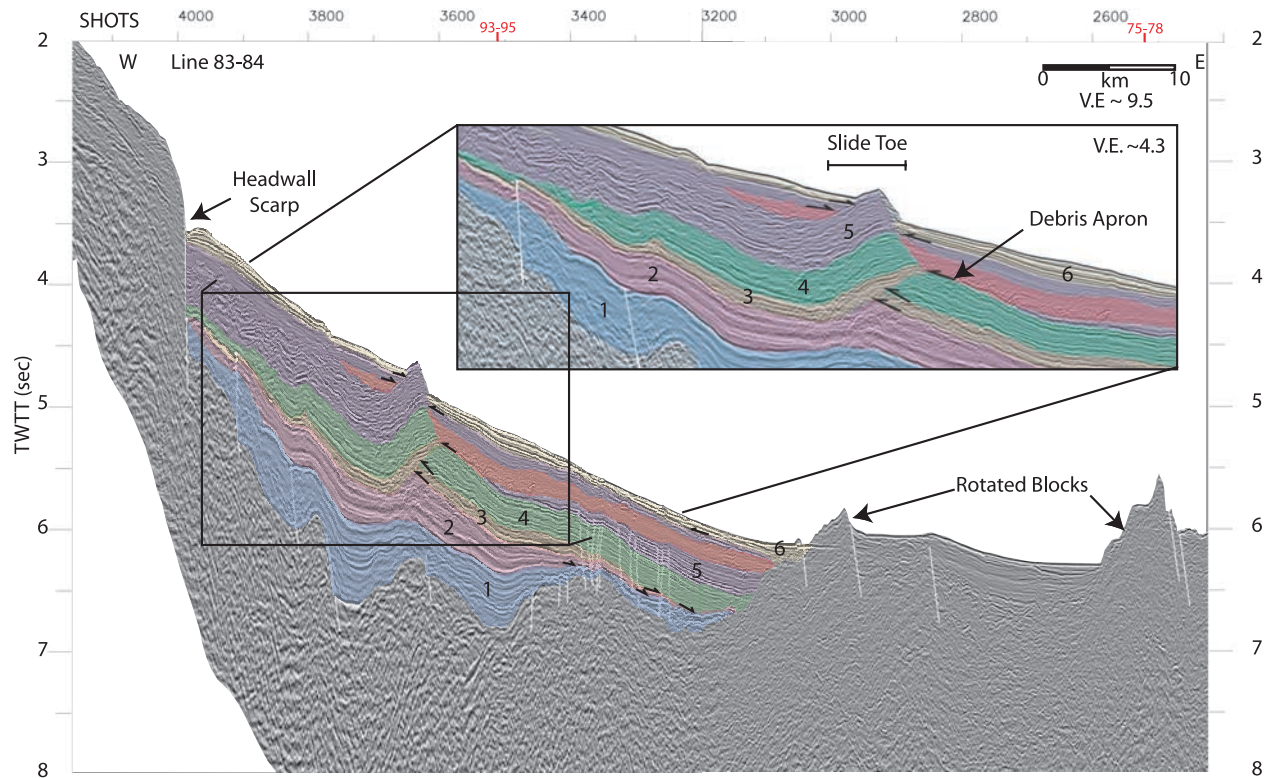


Figure 3. Line 83–84 images the cross section of a submarine landslide in the forearc basin. The thrust toe of the slide, the headwall scarp, and the reworked slide debris around the slide (red sediment) are labeled. Imaging of the rotated basement blocks on the eastern side of the basin show some internal layering, which could reflect layered lava flows.

arcward edge of the basin by normal faults that isolate the perched sediment above the main basin near SP2300. We interpret these perched sediments as Units 1, 2, and 3 based on similarities in seismic character to those of the main basin.

[19] Unit 2 (pink) sediment laps onto Unit 1 on both sides of the main basin. Its lower section is wedge shaped, thins eastward, and appears folded, possibly by midsequence basement inversion near SP2900. The upper section of Unit 2 is composed of layered subparallel reflections on both sides of the basin that drape the underlying section and lap onto the edges of the basin, with differential sedimentation over the midsequence fold. Unit 3 (orange) is subparallel to the upper part of Unit 2 but laps onto Unit 2 in several places. These sediments are thickest toward the arc and make up most of the sediment in the perched basin. Unit 4 sediment (green) is overlapped by Unit 5 (purple) in the western and central portions of the basin, but these units are subparallel to one another on the eastern side of the basin. Both units thicken toward the trench and are characterized by strong, layered reflections in the forearc basin near 15°. Unit 6 is

the youngest sediment deposited in the basin. Seismic data show that in the southern survey region, the majority of sediment from Unit 6 bypasses the slope and pools at the base and west of the eastern rotated bounding blocks in a wedge shape, which thins and onlaps arcward near SP3150. The uniform, parallel reflections comprising most of the basin fill in this region of the forearc are most probably a result of broad turbidite flows fanning out across and along the region sourced from mass wasting of the frontal arc high and explosive eruptions of the volcanic arc.

[20] A large submarine landslide in the southern region, ~15.3°N, 146.2°E, is imaged on Lines 83–84 and 93–95 (Figure 3 and Figure 4, respectively). The thickest section of the slide includes Units 3, 4, and 5 with the slip surface at the base of Unit 3 and slide initiation near the end of deposition of Unit 5 sediment. A cross section of the slide on Line 83–84 shows a thick deposit of slide debris with a distinguishable chaotic seismic character in front of the slide (red section). The toe of the slide consists of a thrust package of Units 3, 4, and 5, that protrudes through the seafloor near SP3650. The

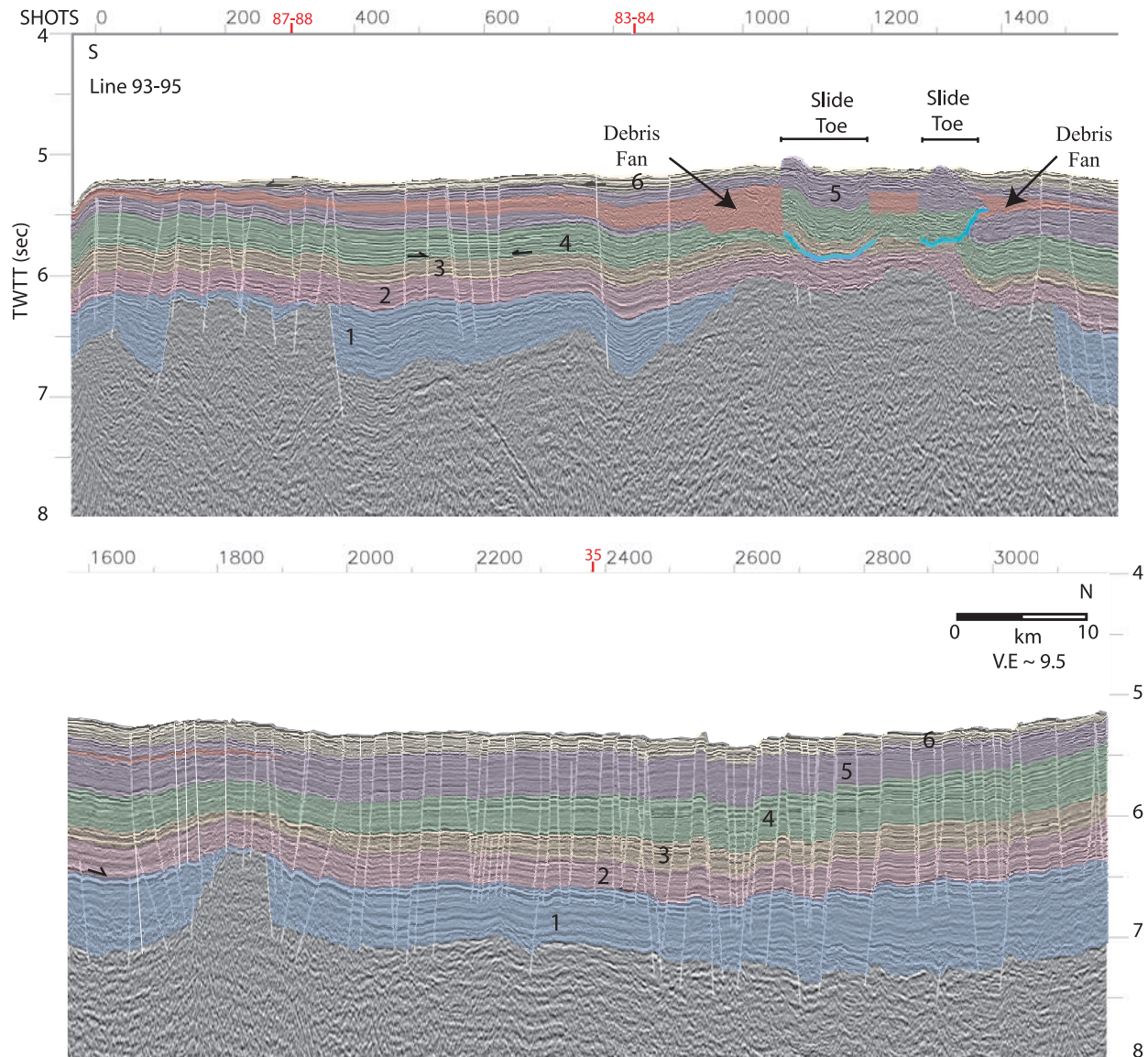


Figure 4. Line 93–95 images the thickness changes of the six seismic stratigraphic units N-S and the toe of the submarine landslide in the southern region of the forearc basin. This line crosses over the toe of the slide in two places (indicated by blue lines) and the sediment in front of the slide. The reworked debris fans off either side of the slide toe can be traced by their chaotic seismic character. Igneous basement is composed of highly irregular faulted blocks along the southern portion of the Line 93–95. Note that the sediment becomes more heavily faulted north of the submarine landslide.

headwall breakaway is imaged as a steep scarp near SP4000. Line 93–95 shows both the toe of the slide and sediment in front of the slide creating a composite out-of-plane image of both depositional environments. The toe is seen in two places from SP1050 to SP1190 and SP1280 to SP1350, and the sediment in front of the slide is best imaged from SP1190 to SP1280. The chaotic sediment fans off either side of the slide creating a debris apron around the toe of the slide (red section). This sediment is significantly thicker to the south than

to the north. The extent of the slide can be seen by following the toe of the thrust in the seafloor bathymetry, which is indicated by the purple line on Figure 1.

[21] Line 93–95 (Figure 4) images changes in unit thicknesses along the southern survey region, which are also illustrated in isopach maps of each unit (Figure 5). Unit 1 thicknesses are highly variable across the southern study area. This Unit most commonly consists of sediment wedges with

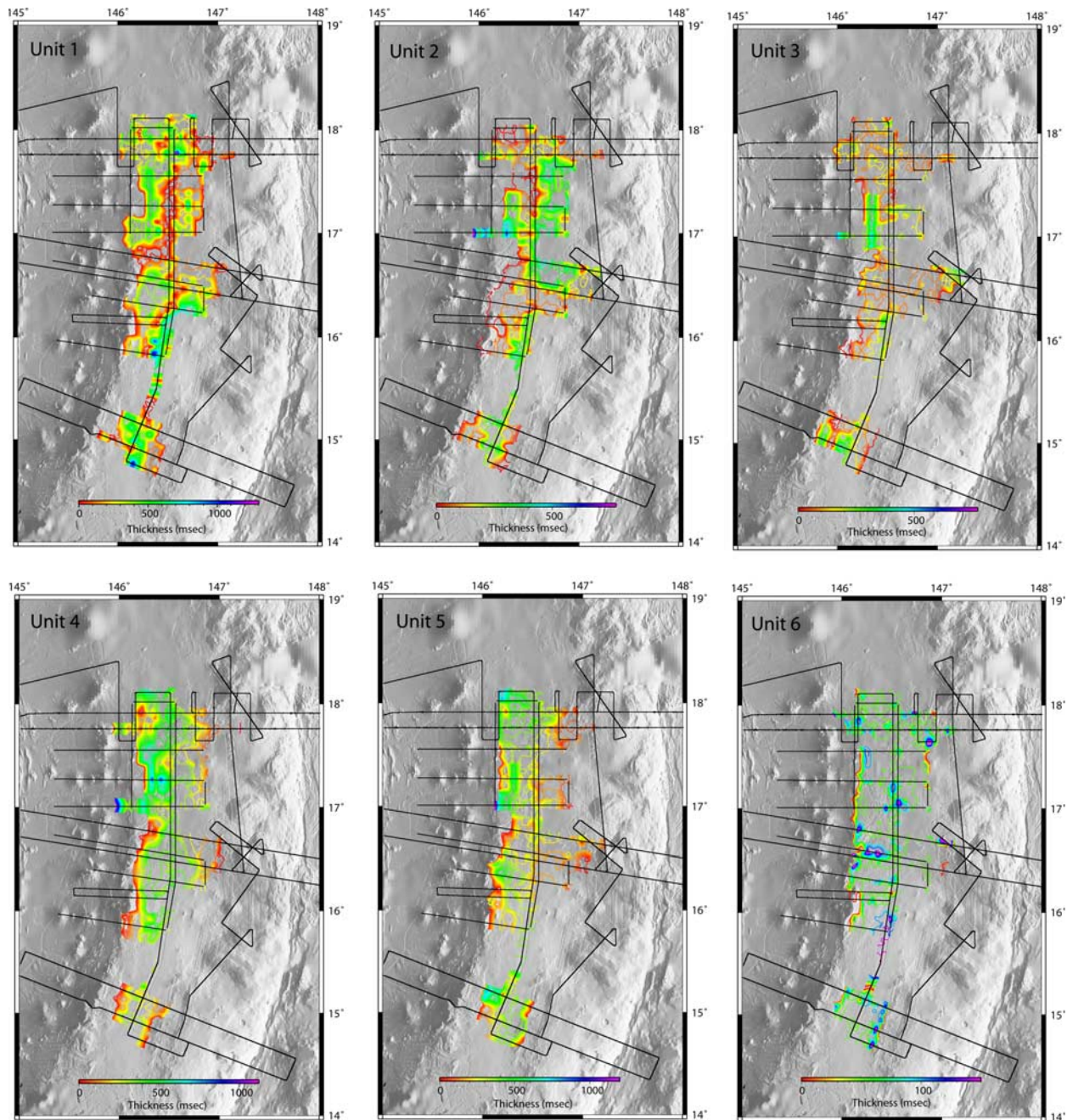


Figure 5. Isopach maps for each of the seismic stratigraphic units calculated in milliseconds of two-way travel time. Sediment thicknesses are color contoured (25 ms contours) with a scale bar in milliseconds on each map. Contours were calculated based on an interpolated 1 km by 1 km grid of sediment thickness with a search radius of 16 km. Overlain on each map are the locations of the seismic lines.

bedding onlapping the tops of faulted basement blocks and is interpreted as syn-rift sediment. Unit 2 gradually thickens to the north, with a maximum thickness within the southern region of ~ 0.3 s. Unit 3 thickens both north of the slide near SP2100 and south of SP350 (Figure 4), as illustrated in the isopach map for Unit 3 (Figure 5c). Unit 4 also thickens near SP2100 and continues to increase in

thickness to the north. In contrast, discounting the area of the slide, Units 5 and 6 thicken toward the middle of Line 93–95 near SP2000.

3.2. The 16.5°N Region

[22] Seismic lines collected in the forearc north of $\sim 16^\circ\text{N}$ are more closely spaced than those further

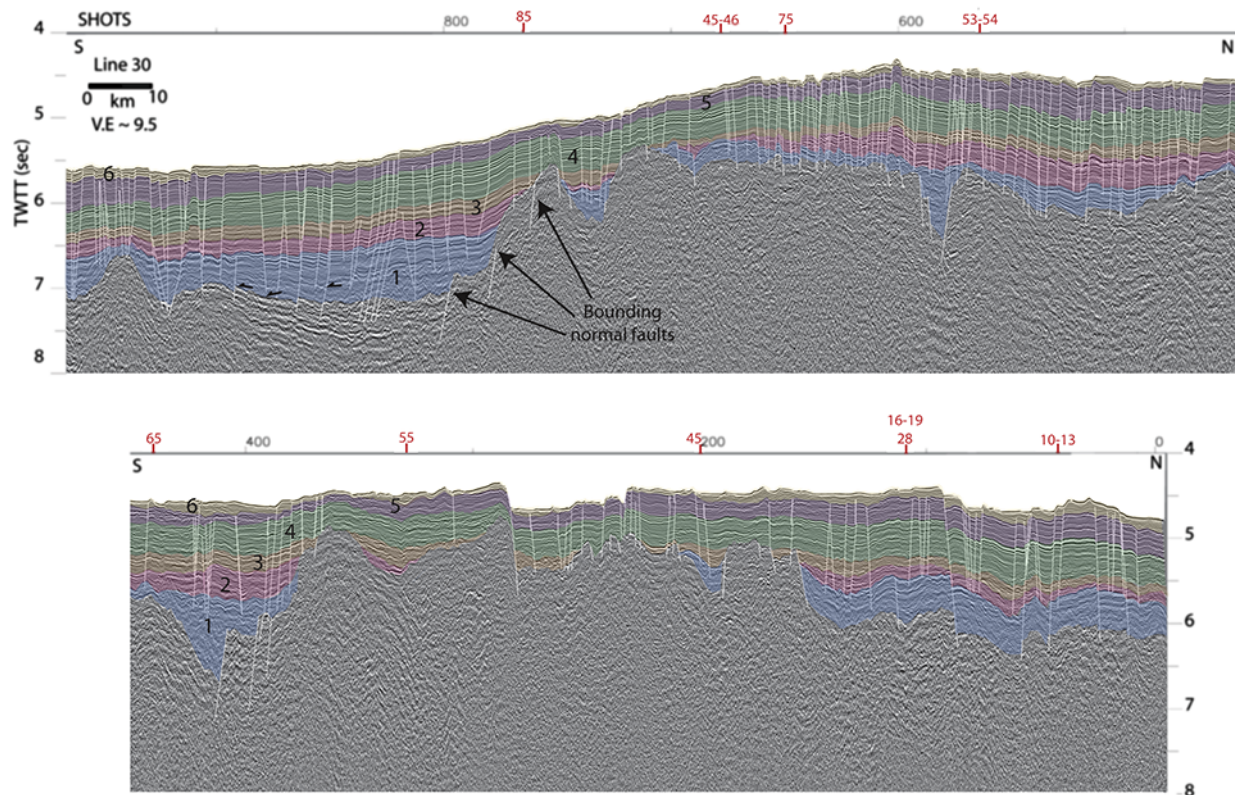


Figure 6. Line 30 images the six sedimentary units from 15.6°N to 18°N and shows the bounding normal faults that offset the deep southern basin from the central basement high. The sediment becomes heavily faulted in the 16.5°N region with numerous high angle normal faults. Large fault-bounded blocks make up the basement over most of the survey region.

south thereby allowing better definition of fault and basement trends. Line 30 runs north along the central and northern regions of the seismic survey and images the sedimentary units across the NW-trending 16.5°N bathymetric high (Figure 6). A series of normal faults (dipping ~40°) between SP750 and SP800 with NE trends mark a transition from the deep southern basin to the thinner sediment cover on a basement high. The edge of this high is illustrated by the NE-trending red contours which form a ridge that extends from 16°N, 146.25°E to 16.5°N, 146.5°E in the isopach map for Unit 1 (Figure 5a). This map shows the abrupt transition between the thick Unit 1 deposits to the south and the absence of this unit on top of the basement fault block highs.

[23] Line 85 (Figure 7), which crosses the forearc at this transition, shows three NE-trending faults offsetting Unit 1 (SP190, SP160, and SP130), which correspond to the normal faults of Line 30 (SP770-SP800). West of these faults lies an undisturbed sequence of Unit 1 sediment, which was

deposited on the flank of the frontal arc high. To the east, Unit 1 is much thicker (Figure 5a). Trenchward of these faults, faulting and tilting after Unit 1 deposition created a ridge onto which Units 2, 3, and 4 onlap. Units 5 and 6 drape over the older sequences across the basin and are continuous over the faulted ridge of Unit 1 sediment. The strong layered reflection characterizing Units 4 and 5 in the 15°N region of the basin is absent here. Instead, the arcward extent of these deposits comprises irregular, hummocky reflections indicative of syn-deposition channel cut and fill. Similar deposits are imaged in the Izu-Bonin forearc to the north [Cooper *et al.*, 1992].

[24] Although Line 85 (Figure 7) is more than 120 km north of Line 87–88, some of the same onlap relationships exist. Units 2, 3, and 4 lap sharply onto the rotated and faulted Unit 1 sediment, though their complete geometry is not imaged before the line ends to the east. Units 3, 4, and 5 are roughly parallel to one another comparable to

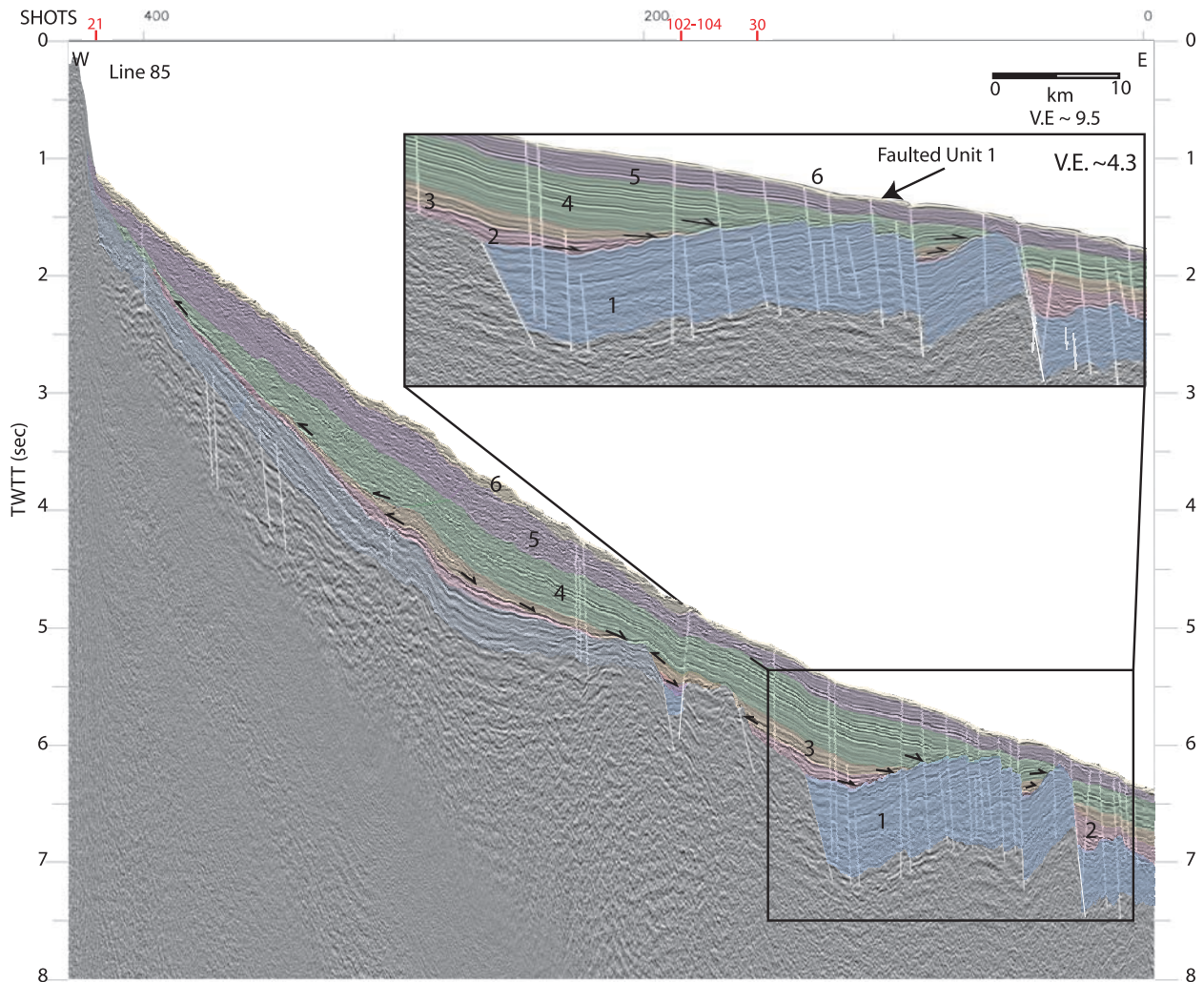


Figure 7. Line 85 shows a cross section of the forearc basin at the transition between the 15°N and 16.5°N regions. Unit 1 sediment becomes heavily faulted east of the tie with Line 30. Units 2 through 6 onlap the faulted Unit 1 sediment noted by black arrows.

Line 87–88; however, Unit 5 thickens to the west on Line 85 but thickens to the east on Line 87–88.

[25] In contrast, Line 53–54 which crosses the forearc basin and the north flank of Celestial Seamount (Figure 1) is representative of a distinctly different geometry observed on the seismic lines across the NW-trending 16.5°N bathymetric high (Figure 8). Line 53–54 images a thinly sedimented frontal arc high slope, with west-tilted fault blocks resulting from trenchward dipping normal faults. The fault blocks continue downslope and beneath the sedimentary basin where both arcward and trenchward dipping normal faults are prevalent. The thickest forearc basin sediment deposits occur east of SP3850. The oldest units are interrupted by a basement high between SP4900 and SP5100, but

east of this high there is a thick sedimentary section containing Units 2 to 6 that continue under the toe of Celestial Serpentinite Seamount near SP5350. The bounding normal faults that created the perched basin on Line 87–88 to the south are not present here.

[26] The forearc basin sedimentary deposits on and north of Line 53–54 are more heavily faulted, and the slope of the basin is less steep, than those further to the south. The high angle faults that offset seafloor and sediment dip between 65° and 75°. The igneous basement of the basin is also composed of smaller offset, more numerous fault blocks than those to the south with average fault dips between 45° and 55°. This trend continues across the central basin and is evident in the

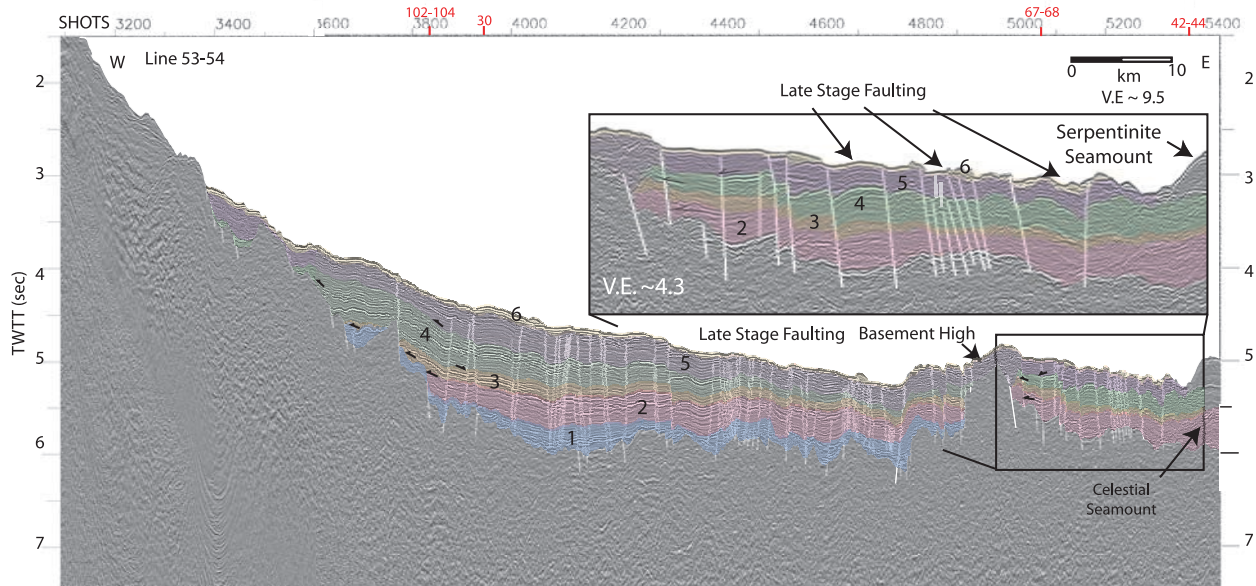


Figure 8. Line 53–54 shows the geometry of the 16.5°N forearc region. The thickest section of the basin is bound on either side by the faulted frontal arc high to the west and a basement high to the east (~SP4900). Sediment is deposited east of this high but coherent reflections are lost beneath the toe of Celestial Seamount, a serpentinite mud volcano. The blowup of the eastern side of the basin shows late-stage faulting east of the main sedimentary basin.

irregular basement imaged on Line 30 across the bathymetric high (Figure 6). These basement irregularities continue north of Line 53–54 toward the thickest section of sediment in this region between SP375 and SP550 on Line 30. Units 1, 2, and 5 become very thick in this area and Units 1 and 2 continue until they onlap a large basement high at SP375 just north of 17°N.

3.3. The 18°N Region

[27] The northern region of the study area has the densest distribution of seismic data and reveals the most complicated basement structure in the forearc surveyed. Large seafloor offsets and basement highs are evident from bathymetric data (Figure 1). Also obvious from bathymetry is the diminished frontal arc high that is subducted north of 17.5°N. Lines 10–13 and Line 16–19 image the complete forearc structure of the 18°N region and are representative of the forearc geometry in this area (Figures 9 and 10, respectively). Although these lines are only ~15 km apart, they show distinctly different features within the northernmost survey area. Line 10–13 images a cross section of the forearc with a basement volcanic high in line with the inferred Eocene arc, whereas Line 16–19 images a broad bathymetric high further west, with internally off-

set reflections overlain by a thick sequence of chaotic sediment.

[28] The frontal arc high in the 18°N region appears absent in the bathymetry; however, Line 10–13 shows a buried volcanic edifice onlapped by Units 1 through 6 sediment centered near SP1950. The forearc basin contains thick sediments bound on the western edge by the volcanic high and the eastern edge by a broad basement ridge. This ridge trends NE across several seismic lines until it becomes obscured beneath Big Blue Serpentine Seamount (Figure 1). An irregular basement composed of numerous rotated normal-faulted blocks makes up the floor of the forearc basin west of the basement high near SP750. Several arcward dipping normal faults offset the main sedimentary basin from thinner deposits on top of the basement high. East of the high, a thin sedimentary sequence lacking distinguishable stratigraphic units covers the basement of the outer forearc, which is composed of numerous rotated blocks.

[29] The DSDP drill sites 458 and 459 are located just south of Line 10–13 along Lines 30–31 and 34–35, respectively (Figure 1; tie locations shown in red, Figure 9). These sites were drilled on the thinly sedimented outer forearc, similar to that

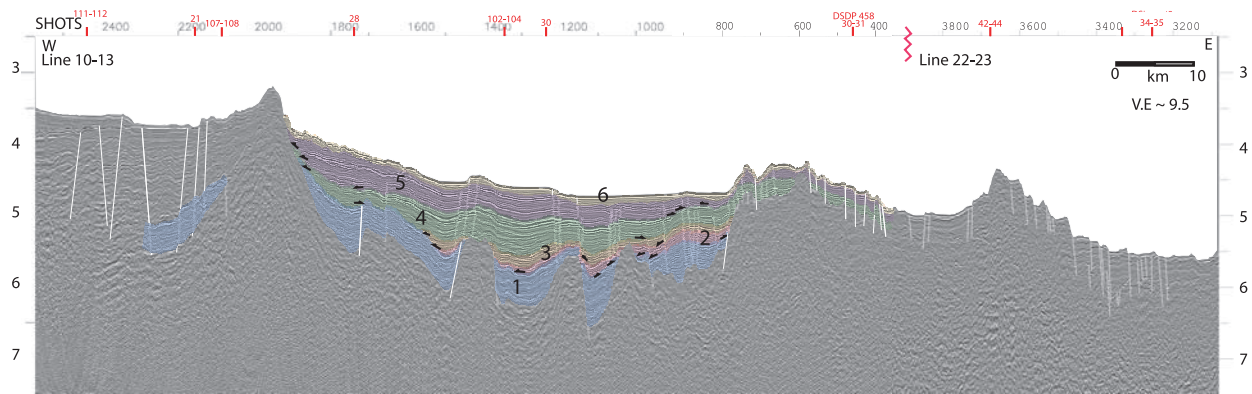


Figure 9. Line 10–13 shows the geometry of the 18°N forearc region with a large volcanic edifice on the western side of the basin. The basement of the sedimentary basin is composed of large, rotated fault blocks. The western side of the basin is bound by a volcanic structure, and the eastern side is bound by a shallow basement high. Seismic interpretations end near SP400 because individual units cannot be traced further east. This line overlaps with Line 22–23 denoted in red.

imaged where Line 30–31 crosses Line 10–13. Drill results for Site 458 show ~10 m of lower Oligocene sediment, ~150 m of lower Oligocene to middle Miocene sediment, ~65 m of middle Miocene to upper Pliocene sediment, and ~28 m of upper Pliocene to Pleistocene sediment [Shipboard Scientific Party, 1978c]. Site 459 was drilled in a thicker sediment deposit similar to the easternmost blocks on Line 10–13. Over 550 m of sediment ranging in age from late Eocene to late Pleistocene were drilled at this site, with only 20 m of sediment dated older than 30 Ma. The oldest seismic stratigraphic sequences (Units 1, 2, and 3) may be present across the outer forearc east of the basement ridge on Line 10–13 (~SP400–SP800); however, these deposits are too thin to be seismically distinguishable.

[30] The volcanic edifice imaged on Line 10–13 does not appear on Line 16–19 (Figure 10). Instead there is a thick deposit of Unit 5 sediment covering a ridge-forming faulted sequence of Units 1 through 4. Further east, Line 16–19 shows an irregular forearc basement composed of rotated fault blocks with thick deposits of Unit 1 sediment between blocks similar to that imaged on Line 10–13. A faulted basement ridge centered near SP10600 to SP10700 interrupts deposition of Units 1 through 3, while younger sediment deposits over this high. Closer to the trench on the eastern side of this high is a complete sequence of Units 1 through 6, showing late stage faulting and rotation from the end of deposition of Unit 5 sediment to the present. The seismic line shows that the seafloor is more heavily offset in the outer forearc than the inner forearc; a trend that is repeated on Lines 10–13

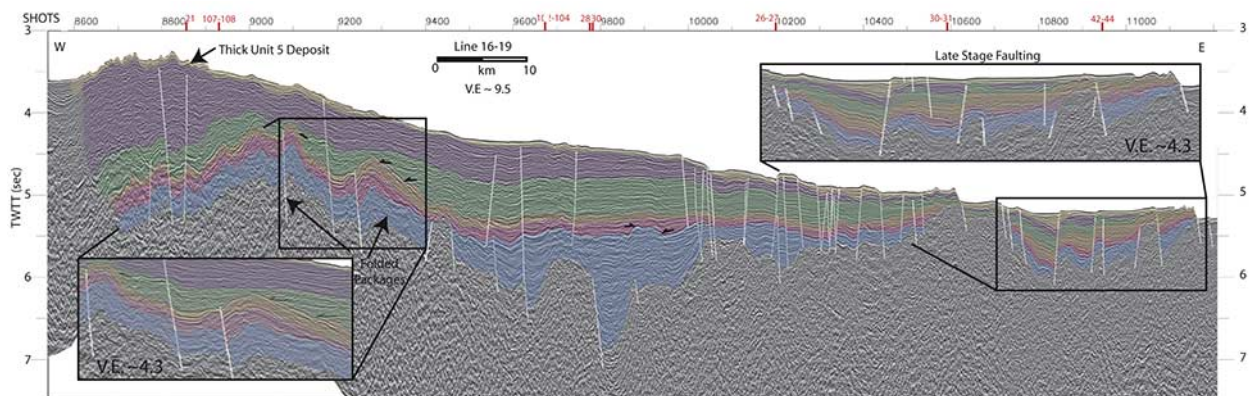


Figure 10. Line 16–19 shows the geometry of the 18°N forearc region with a thick Unit 5 deposit on the western side of the basin. The basement and sedimentary basin are composed of large, rotated blocks. Two reverse fault structures highlighted by the leftmost blowup are imaged on this line. The blowup of the eastern side of the forearc shows late-stage tilting of sediment in the outer forearc.

and 53–54. In addition to this recent deformation, seismic data image two compressional features on Line 16–19 near SP9100 and SP9300. Basement faulting leading to the folding of Units 1, 2, and 3 occurred in the inner forearc between deposition of Units 3 and 4 as evidenced by the onlap of Unit 4 sediment onto Unit 3.

[31] The sedimentary units in the 18°N region have similar onlap relationships to those further south. We interpret Unit 1 sediment as the wedge-shaped to subparallel syn-rift deposits between basement blocks. This unit onlaps the flanks of the volcanic high on the western side of the basin on Line 10–13 and is faulted and buried under thick Unit 5 deposits on Line 16–19. Units 2 and 3 are also deposited during continued normal faulting and onlap Unit 1 in several places across the forearc basin. Units 4 and 5 onlap Unit 1 along the western edge of the basin on Line 10–13, and Unit 4 laps onto Unit 5 on the eastern side of the basin near SP900 (Figure 9). The forearc basin has the lowest surface slope in the northern survey area.

[32] Two other seismic lines also image mild compressional features in the northern survey region between 17° and 18°N. Line 55 reveals the most severe compression; a large anticline structure of folded Units 1 through 4 sediment centered near SP540 (Figure 11a). This anticline was created from compression of sediment deposited between two basement highs. By flattening the boundary between Units 3 and 4, we are able to look at the unfolded sediments of Units 1, 2, and 3 (Figure 11b). This view shows two half grabens filled with Units 1, 2, and 3 which are offset by a steep normal growth fault. We interpret the anticline to have formed by reverse movement on this normal fault after deposition of Unit 3 sediment. Once the fault reversed, Units 1, 2, and 3 on the trenchward side of the fault were uplifted while Unit 4 deposition and folding occurred contemporaneously. Unit 4 sediment forming the crest of the anticline was eroded, leaving an angular unconformity between Units 4 and 5 from ~SP540 to SP600 (Figure 11a). Unit 5 and 6 sediment was deposited on top of the eroded anticline after reverse faulting had ceased.

[33] We see a similar structure on Line 65 as a folded sequence of Units 1 through 4 between SP275 and SP310 (Figure 11c). While there is a basement high on the trenchward side of the structure like that on Line 55, to the west there is a thick section of faulted sediment beneath a broad bathymetric high like that is imaged on Line 16–19. Since the fold structure on this line is similar to

that of Line 65 but less severe, we interpret the two lines to show a single NW-trending anticline. The extent of this structure is illustrated in the isopach map for Unit 4 (Figure 5d). Seismic data show another smaller reverse fault just west of the large anticline on Line 65 near SP350 (Figure 11c). Folded sediment from Units 1 through 3 was uplifted on the western side of an arcward dipping fault. Unit 4 sediment does not appear as folded as older units, and Units 5 and 6 are unaffected by the inferred reverse faulting of the basement.

4. Discussion

4.1. Seismic Stratigraphic Units

[34] The six seismic stratigraphic units mapped across the inner Mariana forearc from 14.5°N to 18.5°N show that the amount of faulting and rotation and the thicknesses of these units vary across the survey region. These differences can be used to distinguish the magnitude and extent of both sediment deposition and strain accommodation that occurred in the forearc. We will discuss the seismic stratigraphic units from oldest to youngest. Table 1 summarizes each stratigraphic unit by proposed age, tectonic environment, and seismic observations across the three regions of this study.

4.1.1. Unit 1: Upper Eocene to Lower Oligocene

[35] Unit 1 deposits are characteristically syn-rift wedge-shaped deposits in half grabens, with bedding subparallel to and onlapping rotated basement blocks. The presence of this sediment throughout the forearc indicates that the rifting that occurred during deposition of Unit 1 affected the entire survey region, hereafter referred to as Unit 1 rifting. The thickest deposits of Unit 1 sediment are located in the forearc basin to the south from 14.5°N to 16.3°N and in isolated half grabens from 17°N to 18°N (Figure 5a). In both regions, the differential sedimentation and stratigraphic rotation across basement-offsetting normal faults (including those offsetting the perched basin on Line 87–88) show that faulting was active during deposition of Unit 1.

Unit 1 sediment is absent on the crests of basement blocks, rotated in the footwall of large-offset normal faults, and is regionally thinnest on the NW-trending basement high near 16.5°N as illustrated by the red contours on Figure 5a. Igneous basement in the 16.5°N survey region remained relatively high when thick Unit 1 sediment was deposited in adja-

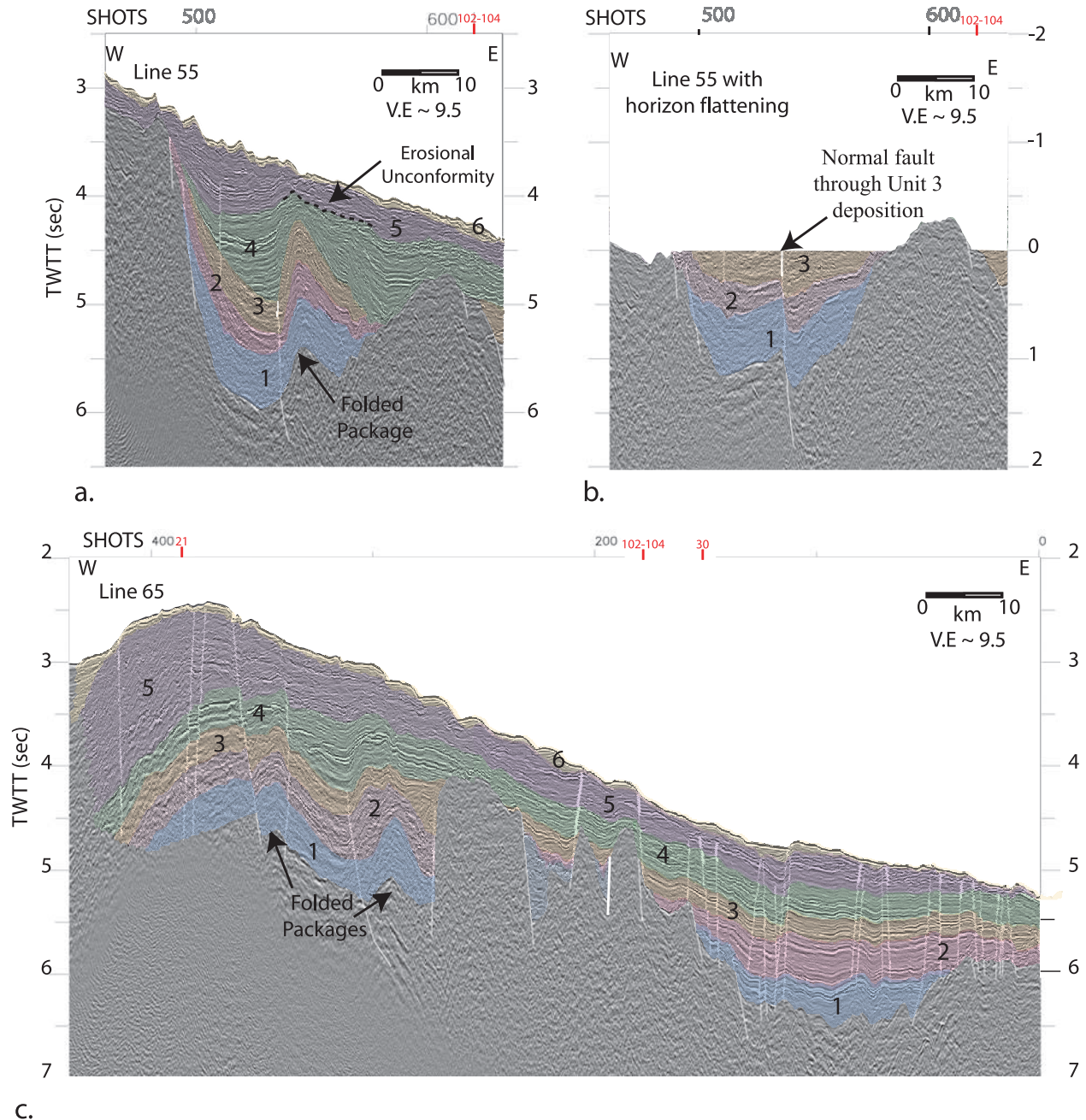


Figure 11. (a) Line 55 shows an anticline composed of folded sediment from Units 1 through 4. (b) Line 55 with horizon flattening of the boundary between Units 3 and 4 shows a normal fault offsetting the oldest units. The normal fault in the flattened seismic line indicates that the anticline was created by reverse motion on this normal growth fault. (c) Line 65 shows a less severely faulted section of the anticline. Units 1 through 4 are deformed in a similar structure to those of Line 55. Another smaller inversion structure is imaged on Line 65 just west of the anticline.

Table 1. Summary of Each Stratigraphic Unit, Associated Arc Stage, and Regional Observations^a

	Unit 1	Unit 2	Unit 3	Unit 4	Unit 5	Unit 6
Proposed age	35–29 Ma	35–29 Ma	35–29 Ma	29–8 Ma	29–8 Ma	8 Ma to present
Arc stage	Eo-Oligocene volcanism with early stage forearc rifting	Eo-Oligocene volcanism with middle stage forearc rifting	Eo-Oligocene volcanism with late stage forearc rifting	volcanic lull after Eo-Oligocene through Miocene volcanism	volcanic lull after Eo-Oligocene through modern arc volcanism	modern arc volcanism
15°N region observations	syn-rift deposits	syn-rift deposits with mild compression	syn-rift deposits	sediment accumulation	forearc subsidence and submarine landslide	accelerated subsidence and trenchward tilting
16.5°N region observations	absent	syn-rift deposits	syn-rift deposits	sediment accumulation	renewed extensional faulting	continued extensional faulting
18°N region observations	syn-rift deposits	syn-rift deposits	syn-rift deposits	sediment accumulation with reverse faulting and compression	renewed extensional faulting	continued extensional faulting

^aRegional constraints on the geologic evolution allow us to consider the proposed age assignments for the seismic stratigraphic units.

cent subsiding basins. This is true of most of the NE- and NW-trending basement highs that cut across the forearc region.

4.1.2. Unit 2: Upper Eocene to Lower Oligocene

[36] Seismic data show that rifting occurred in the forearc during deposition of Unit 2 sedimentation, hereafter referred to as Unit 2 rifting. The sediments, as interpreted from the stratigraphy, deposit over the syn-rift layers of Unit 1, and in many cases lap onto the most heavily rotated deposits of Unit 1 sediment. The extent of Unit 2 deposits, however, appears more limited than that of Unit 1, indicating that many of the earliest formed rift basins did not continue as depocenters after Unit 1 accumulation.

[37] Unit 2 rifting was less dramatic than that of Unit 1 in the Mariana forearc and involved motion on some of the same large fault systems that were active during Unit 1 rifting. Seismic data show that in addition to motion on these older fault systems, Unit 2 rifting also involved initiation of several new faults, like those in the 16.5°N region. The eastern end of Line 53–54 shows several basement-offset faults created during Unit 2 rifting, as well as faulting that occurred later in the forearc basin (Figure 8).

[38] In addition to the extension during Unit 2 deposition (discussed above), local compression also occurred in the 15°N region of the forearc during the accumulation of Unit 2 sediment. Line 87–88 shows a compressional structure of folded sediments of Units 1 and 2 near SP2800 (Figure 2). While compression is seen in the northern survey region during Unit 4 deposition, Line 87–88 images the earliest example of compression in the Mariana forearc basin. This folding above an inferred reverse basement fault is a local event since it is not imaged on Lines 91–92 or 83–84 which are less than 2 km and 5 km to the south and north, respectively.

4.1.3. Unit 3: Upper Eocene to Lower Oligocene

[39] Unit 3 sediment thickness changes across several normal faults indicate that rifting continued during this period, though it was not as extensive as that during deposition of Units 1 and 2. The forearc basin in the 15°N region, imaged on Line 87–88, experienced Unit 3 rifting (Figure 2). The increase in sediment thickness on

the western side of the main sedimentary basin is a reverse trend to that of Units 1 and 2, which increase in thickness to the east. Although this depositional pattern could be caused by a change in sediment source, we suggest that it is a result of continued motion on the fault system separating the main and perched basins during deposition of Unit 3. This fault motion resulted in a thick deposit of sediment in the western main basin and created a significant fault scarp by the start of Unit 4 deposition (which bypassed the perched basin). This extension is also imaged on several seismic lines across the 16.5°N and 18°N regions, which show normal faulted basement blocks offset during Unit 3 rifting.

4.1.4. Unit 4: Upper Miocene to Lower Pliocene

[40] Unit 4 sediment has a fairly uniform thickness (0.4 s two-way travel time) within the forearc sedimentary basin except for local areas of thicker deposits between 17°N and 18°N. This uniformity is notable because it shows that the earlier rift graben depocenters no longer controlled deposition by the time of Unit 4 accumulation. Instead, sediment was deposited within a large forearc basin bounded by the frontal and outer arc highs. Seismic data show that localized thickening is a result of compressional structures created in the forearc predominantly during Unit 4 deposition. In many cases, this compression results from inversion of normal faults that were active during Unit 3 rifting (Figure 12). The locations of these thicker deposits resulting from compression are indicated by the blue contours on Figure 5d. The isopach map also shows the regionally uniform deposit of Unit 4 around these structures, marking the extent of the forearc sedimentary basin during this time.

4.1.5. Unit 5: Upper Miocene to Lower Pliocene

[41] Unit 5 deposits have variable thickness throughout the Mariana forearc and lap onto Unit 4 in many places across the basin. Relative forearc subsidence near 16.3°N began during deposition of Unit 5. This subsidence is obvious on Lines 87–88 and 83–84, which show trenchward thickening deposits of Unit 5 sediment (Figures 2 and 3). This thickening is imaged on all three trench-perpendicular lines collected in the 14.5°–15°N region of the forearc. There is no evidence for subsidence in the forearc on or north of Line 85 during Unit 5 deposition. Instead, the seismic lines north of Line

85 show Unit 5 sediment thinning steadily eastward across the outer forearc.

[42] Our seismic stratigraphic analysis indicates that subsidence in the 15°N region continued through the end of Unit 5 deposition. This is also the time of the submarine landslide imaged on Line 83–84 and Line 93–95 (Figures 3 and 4). The slide includes sediment from Units 3, 4, and 5. On the basis of the time of slide initiation (late Unit 5) and the geometry of the slide, we infer that this landslide was generated from slope instability triggered by differential subsidence of the southern forearc and/or uplift of the frontal arc high. The detachment scarp is located parallel to the western basin bounding faults on Line 87–88 that separate the perched and main sedimentary basins. We conclude that the preslide geometry of Line 83–84 was similar to that imaged on Line 87–88 and that the slide detached from the western bounding faults.

[43] The isopach map for Unit 5 shows very thick deposits close to the modern arc near 17°N and 18°N (Figure 5e). Lines 65 (Figure 11c), and 16–19 (Figure 10) show typical seismic cross sections of the thick Unit 5 deposit. A broad, low relief accumulation of sediment is imaged on both seismic lines with faulted sediment of Units 1 through 4 beneath the sequence. It is likely that the source of the Unit 5 sediment was a volcano proximal to these seismic lines, which would explain the dramatic thickness increase.

[44] Fault patterns and stratal offsets indicate that renewed extension of the forearc began near the end of Unit 5 deposition and is currently active. The most heavily faulted areas of the inner forearc observed on the two north-trending Lines 93–95 and 30 (Figures 4 and 6) are between 15.5°N and 17°N.

[45] The extent of Unit 5 deformation in the 15°N and 18°N regions of the survey appear similar from seismic data and less dominant than the intervening regions discussed above. Seismic data show high angle normal faults offsetting sedimentary Units 1 through 5, and in many cases, Unit 6. These faults dip between 65° and 75° and appear more prevalent in the outer forearc, suggesting that the most recent deformation affected the outer forearc more than the inner forearc.

4.1.6. Unit 6: Lower Pliocene to Present

[46] Unit 6 deposits comprise a thin blanket of sediment with variable thickness across the forearc. The thickest deposits of Unit 6 are only ~0.1 s of

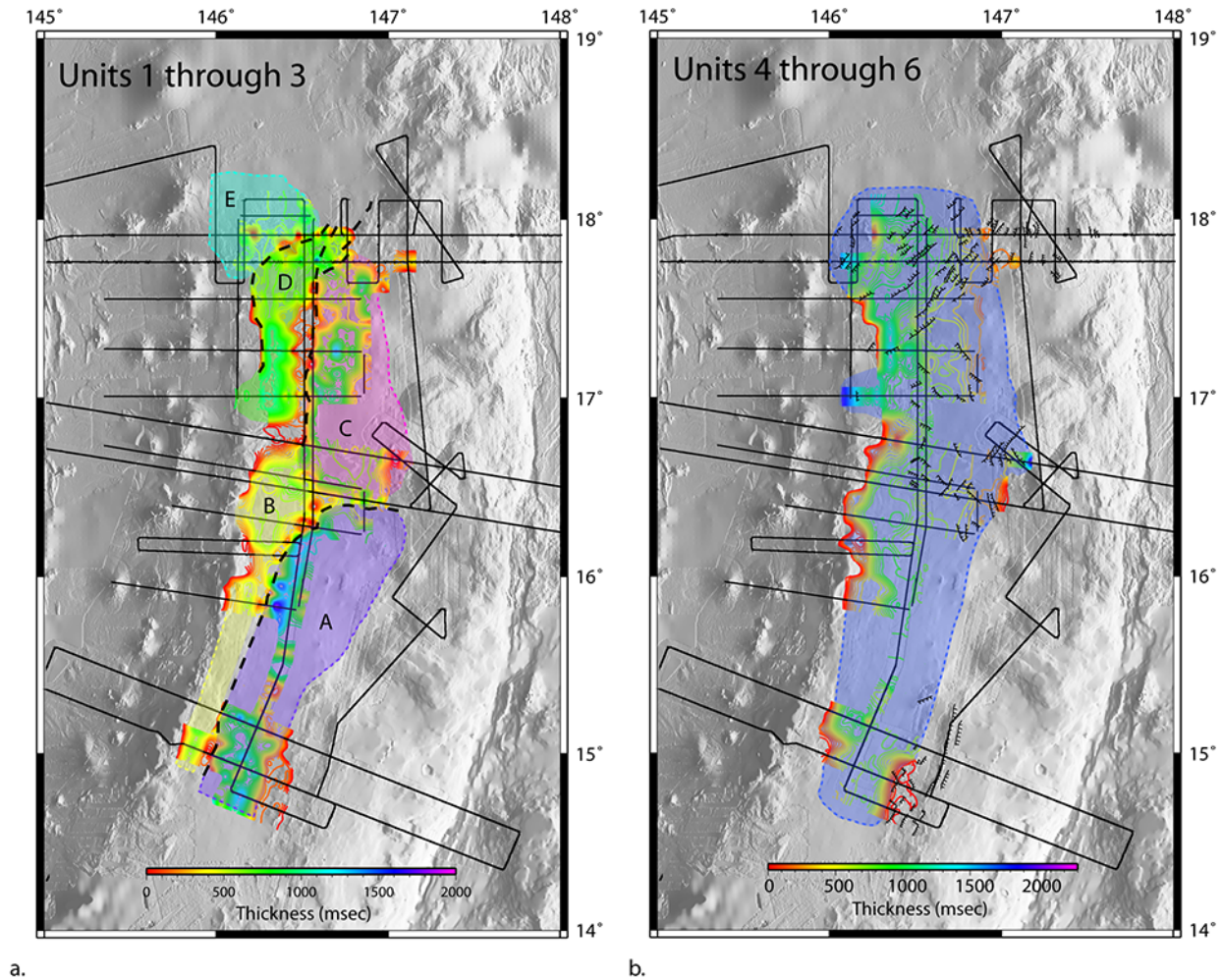


Figure 12. (a) Isopach map showing the cumulative thickness of Units 1 through 3 across the survey region during Eo-Oligocene rifting. Individual depocenters for sediment accumulation are labeled A–E and shaded in color. Dashed, colored lines around the perimeter of individual basins denote areas of inferred basin boundaries and/or the limit of seismic data. Black dashed lines indicate locations of large, trenchward dipping fault systems active during deposition with north to, and NNE trends. (b) Isopach map showing the cumulative thickness of Units 4 through 6 across the survey region from ~29 Ma to the present. Modern fault locations that could be correlated between seismic data and bathymetry are drawn in black showing dominant NE, NW, and NNE trends for recent extensional deformation. Blue shading indicates a single depocenter for sediment accumulation as opposed to numerous localized basins during accumulation of Units 1 through 3.

two-way travel time compared to an average thickness of ~0.4 s for the other seismic stratigraphic units. Since Unit 6 is the youngest sedimentary unit and volcanism is occurring on the Mariana Arc today, we infer that Unit 6 includes volcanoclastic sediment currently depositing in the forearc. Extensional deformation that occurred in the forearc during Unit 6 deposition is still ongoing, with seafloor-offset faults visible throughout the forearc. This faulting appears to be a continuation of Unit 5 deformation as many of the faults initiated during Unit 5 sediment accumulation show continued movement during Unit 6 deposition. The most

heavily faulted areas are those described above for Unit 5, including increased faulting of the outer forearc. The thickest deposits of Unit 6 sediment are in these heavily faulted areas implying deformation and deposition were and are occurring simultaneously. The regional extent of Unit 6 deposits suggests that sediment accumulation occurred across the entire forearc basin as older localized depocenters have been infilled.

[47] Accelerated subsidence and rotation of the southern forearc basin near 15°N occurred during Unit 6 deposition. This is evident from the slope-bypassed deposits imaged on Lines 87–88 and

Table 2. Percent Extension Accommodated by Basement Faults Calculated by Measuring Horizontal Offset Across Faults

Line Number	Total Length (km)	Total Fault Offset (km)	Percent Extension
91–92	62.6	2.4	3.8%
87–88	108.4	7.9	7.3%
83–84	88.2	2.8	3.2%
93–95	161.3	2.0	1.3%
53–54	118.3	2.3	2.0%
65	86.9	3.4	3.9%
45	75.7	2.8	3.7%
30	389.2	7.5	1.9%
16–19	133.6	3.8	2.8%
10–13	82.2	4.9	5.9%
			Mean = 3.6%

91–92 (Figures 2 and 3). Subsidence and trenchward tilting of the southern forearc increased during Unit 6 deposition, resulting in sediment bypassing the inner slope and ponding against the bounding rotated basement blocks to the east.

4.2. Dating Seismic Stratigraphic Units

4.2.1. Units 1 Through 3: Upper Eocene to Lower Oligocene

[48] The seismic lines for this study were located in an attempt to tie the seismic stratigraphy to the cores recovered and dated from DSDP Sites 458 and 459 (Figure 1). Unfortunately, intervening basement highs (e.g., Figure 9) make tenuous all but the most general correlations. Nevertheless, regional constraints on the geologic evolution allow us to consider some reasonable age assignments for the seismic stratigraphic units. The initiation of the IBM and other western Pacific convergent margins ~ 50 Ma instigated the reorganization of several large tectonic regimes in the Pacific including a change in Pacific Plate motion evident from the Hawaiian-Emperor bend and other hot spot traces [Sharp and Clague, 2006]. Several theories have been proposed to explain this plate restructuring including rapid subduction of the Pacific-Izanagi spreading ridge [Whittaker *et al.*, 2007]. Models of hot spot wandering also indicate a southward wander of the Hawaiian hot spot related to changes in mantle flow near the time of IBM initiation [Koppers and Staudigel, 2005; Tarduno, 2007]. Another major tectonic restructuring was the rotation of the West Philippine Basin opening from a NE-SW to a N-S spreading direction. It is hypothesized that this spreading west of the initial Mariana volcanism resulted in massive along-strike stretching of the forearc region

[Sdrolias *et al.*, 2004; Taylor and Goodliffe, 2004]. This extension was coeval with suprasubduction “ophiolitic” volcanism creating a stretched boninite tholeiite forearc basement overprinted by seafloor eruptions and intermittent volcanic highs. It is uncertain whether early volcanism included subareal eruptions that would create volcanoclastic deposits in the forearc. If these deposits do exist, however, they would be interlayered with lava flows and pillow basalts. The middle Eocene sediment at Sites 458 and 459 is very thin (~ 10 m at both sites). Therefore, although it is probable that sediment from the middle Eocene exists across the forearc, these deposits may be thin and indistinguishable in the seismic data.

[49] In considering the age of the syn-rift deposits of Units 1 through 3, we calculated the amount of extension observed in the seismic data from basement faults by measuring the horizontal offset across these faults. Total extension values averaged $3.6\% \pm 0.1\%$ accommodated by faults observed to offset basement (Table 2). This amount of stretching is insignificant relative to the ~ 1000 km of N-S extension proposed to have occurred during the early construction of the forearc region. We conclude that Units 1 through 3 were not deposited during this hypothesized middle Eocene stretching and must have been deposited some time after the formation of the forearc basement.

[50] Continued plate convergence eventually lead to the formation and localization of an organized upper Eocene and lower Oligocene volcanic arc [Taylor, 1992]. This is the first island arc-building phase in the history of the Mariana subduction zone and likely the first major sediment source to the forearc basin. Explosive subareal volcanism peaked during early Oligocene arc rifting, which transitioned to backarc spreading in the Parece Vela

Basin and subduced arc volcanism by ~29 Ma [Scott and Kroenke, 1983]. We propose that Units 1, 2, and 3 were deposited during this upper Eocene to lower Oligocene Mariana arc volcanism and rifting (~35 Ma to 29 Ma).

[51] This timing of the Eo-Oligocene rifting and presumed sedimentary deposits is supported by drilling and seismic survey results from the Izu-Bonin and Mariana convergent margins. The Izu-Bonin arc-trench system along strike to the north has a similar subduction initiation history. Seismic surveys and drilling results in the Izu-Bonin forearc confirm that the first significant forearc sedimentary basin accumulation occurred during Eo-Oligocene rifting ~31 Ma [Shipboard Scientific Party, 1990a, 1990b, 1990c; Taylor, 1992]. With similarities in early histories, one might expect the Mariana system to have an equivalent sedimentary record to the Izu-Bonin margin with maximum sedimentation rates commencing during the late Eocene to early Oligocene rifting. Given the prior onset of backarc spreading in the Mariana versus Izu-Bonin segments, earlier rifting onset may be expected in the Marianas as well, supporting the proposed age of sediment accumulation initiation between 35 Ma and 29 Ma in the Mariana forearc. DSDP sites 458 and 459 in the Mariana forearc also support this hypothesized age of initial sedimentation with both drill cores showing significant sediment deposition established by at least 35 Ma [Shipboard Scientific Party, 1978c, 1978d]. DSDP site 448 on the Palau-Kyushu remnant arc also shows thick sedimentary deposits from the Eocene arc established by 34 Ma, supporting a proposed age for Units 1 through 3 between ~35 and 29 Ma [Shipboard Scientific Party, 1978b].

[52] Units 2 and 3 also accumulated during this period of rifting; however, seismic data show that the amount of extension in the forearc decreased during deposition of Units 2 and 3, likely becoming focused in the arc/backarc. We propose that these units deposited during the later stages of the Eo-Oligocene rifting. Seismic interpretation of three distinct stratigraphic packages suggests this rifting was punctuated by periods of less active faulting, creating the three syn-rift deposits of Units 1, 2, and 3.

4.2.2. Units 4 Through 6: Upper Miocene to Present

[53] Drill sites and island outcrops reveal a volcanically quiet period existed in the forearc after Eo-Oligocene arc rifting ended and before the Miocene

arc was established (~29 Ma and 20 Ma) [Shipboard Scientific Party, 1978c, 1978d; Taylor, 1992]. After the Miocene arc was created (~20 Ma), late Mio-Pliocene arc rifting eventually led to the opening of the Mariana Trough backarc basin (~8 Ma), which is currently undergoing seafloor spreading [Martinez et al., 1995; Martinez et al., 2000]. We propose that Units 4 through 6 were deposited between the end of the late Eocene to early Oligocene rifting and the present (~29 Ma to present). These deposits include any sediment from the late Oligocene volcanic lull and volcanoclastic accumulations from both the Miocene and modern volcanic arcs.

[54] Units 4 and 5 comprise the majority of sediment deposited since Eo-Oligocene rifting ceased in the forearc. These thick deposits probably source from the Miocene arc which was active between ~20 Ma and 8 Ma. By the time Unit 4 sediment was being deposited, high angle reverse faulting of previous normal faults was occurring in several places across the forearc. This phenomenon has been observed to occur on rifted continental margins during subsequent seafloor spreading [Letouzey, 1990]. With the exception of the Unit 4 deposits thickened from inversion, sediment accumulation was fairly consistent in the forearc basin between the frontal and outer arc highs. During deposition of Unit 5 sediment in the forearc basin, southern forearc subsidence began, and near the end of accumulation, extensional deformation in the form of high angle normal faulting (65° to 75°) had begun. These more recent syn-deformation deposits are different than the syn-rift deposits of Units 1 through 3. Unit 5 sediment is disrupted by numerous small offset faults as opposed to the rotated and wedge-shaped deposits of the older syn-rift sediment. Thick deposits of Unit 5 are imaged close to the current arc in the northern region, likely indicating deposition from a nearby volcanic sediment source.

[55] We are unable to correlate the boundary between Units 4 and 5 with a specific volcanic or tectonic event; however, Unit 5 laps onto Unit 4 across the entire survey region suggesting that a regional event occurred in the Mariana forearc. This boundary might indicate a change in sediment source or possibly a sedimentary hiatus across the forearc region. A shifting sediment source seems unlikely as this onlap relationship is defined across the entire survey region requiring a uniform along strike change in each point source volcano across the 450 km survey region. A sedimentary hiatus

observed at Mariana forearc DSDP sites 458 and 459 from 13 Ma to 15 Ma may account for the stratigraphic boundary [*Shipboard Scientific Party*, 1978c, 1978d].

[56] The extensional deformation occurring near the end of Unit 5 deposition continues through Unit 6 accumulation. Current GPS data show that the entire Mariana arc-trench system, including the forearc, is experiencing nonrigid deformational strain associated with the opening of the Mariana Trough [*Kato et al.*, 2003]. The deformation imaged in the seismic data near the end of Unit 5 accumulation and throughout Unit 6 could be a result of this nonrigid deformation beginning ~8 Ma. Seismic data shows that the inner forearc at 16.5°N region is currently experiencing an increased amount of extension relative to the north and south.

4.3. Structural Inversion

[57] The phenomenon of structural inversion is identified in rifted regions throughout the world [e.g., *Letouzey*, 1990; *Terrinha et al.*, 2002]. In many cases of inversion, a large rifting event is followed by a “quiet” period of relatively inactive tectonics preceding reversal of extensional structures, accommodating compression and shortening. Such is the common case when continental extension leads to igneous breakup followed by inversion once seafloor spreading begins.

[58] There are several seismic lines in the inner forearc that show structural inversion occurring during deposition of Unit 4 sediment. Assuming the interpreted ages for forearc sediments discussed above, inversion occurred some time after Eo-Oligocene rifting ceased (~29 Ma). The major inversion structures on Lines 55, 65, and 16–19 involve reverse movement of basement-offset faults, with compression achieved through large-scale reverse faulting of the forearc basement and folding of its sedimentary cover. These structures are located on or very near to the frontal arc high, which is the remnant Eo-Oligocene arc. The most dramatic compressional structure is imaged on Line 55 (Figure 11a). Figure 11b shows a section of the seismic data with the boundary between Units 3 and 4 flattened. This exercise illustrates the pre-reversal geometry, which includes a normal growth fault offsetting Units 1 through 3 that reversed motion after Unit 3 rifting. This example of inversion created a large anticline that is also imaged on Line 65 (Figure 11c). The NW-trending

anticline shows offset of more than one second of two-way travel time across the reverse fault. Assuming an average velocity of at least 2 km/s for the anticline sediments yields more than kilometer of offset on the reverse fault.

[59] A similar flattening exercise verifies that the reverse fault directly west of the anticline and those imaged on Line 16–19 also resulted from inversion of normal growth faults initiated during Unit 1 rifting. Several smaller, less dramatic examples of normal fault reversal are seen on several of the seismic lines across the forearc basin affecting the same sedimentary units.

[60] It is possible that back-arc spreading in the Parece-Vela Basin caused the structural inversion imaged on seismic lines. Dating by magnetic anomalies suggests that seafloor spreading in the backarc basin started 29 Ma with an E-W spreading direction [*Mrozowski and Hayes*, 1979; *Okino et al.*, 1998]. This changed to a NE-SW spreading orientation with a dramatic decrease in spreading rate by ~20 Ma with spreading completed by 15 Ma [*Sdrolias et al.*, 2004]. We propose that inversion occurred in the Mariana forearc sometime between ~29 Ma and 15 Ma during the time of seafloor spreading in the Parece-Vela Basin. The cause of the isolated example of structural inversion on Line 87–88 during Unit 2 deposition is not apparent.

4.4. Forearc Extension

[61] Earliest faulting in the Mariana forearc resulted from north-south stretching of the entire arc-trench system in the Eocene, which we do not see evidence for in the seismic data. A second rift phase in the late Eocene to early Oligocene overprinted whatever extensional structures were created during ophiolitic volcanism, which involved massive eruptions of boninite and tholeiite lavas that formed in the Mariana forearc. We suggest that the primary fault structures of the forearc basin formed during the late Eocene to early Oligocene rifting. Faulting on the trenchward side of the Eo-Oligocene arc occurred across the survey region, leaving a subsided forearc floor for sediment accumulation. The numerous rotated blocks and half grabens making up the forearc basement across the survey region are the structural remnants of this basin-wide extension. This proposed mechanism for forearc basin formation in the Mariana arc-trench system is the same as that believed to have occurred in the Izu-Bonin margin to the north.

[62] There are two different fault sets from this period of extension; a trench-parallel NNE set of faults and an orthogonal set of NE- and NW-trending faults. The dashed lines in Figure 12a show the interpreted trend of the major bounding normal faults across the forearc basin and the resulting depositional pattern of Units 1 through 3. During rifting and deposition, motion on major fault systems (dashed black lines) created basement highs devoid of sediment and depositional lows containing thick deposits. These fault systems trend north/north-northeast and are composed of trenchward dipping normal faults. This image also shows a color-contoured isopach map of the cumulative thickness of Units 1 through 3 as well as local depocenters of sediment accumulation (A through E). The localized depocenters of Units 1 through 3 preceded the uniform sedimentary basin of the current Mariana forearc, which extends from the frontal arc high to the outer arc high.

[63] Figure 12a shows that the fault system in the 15°N region separates the main sedimentary basin in the south (depocenter A) from the perched basin imaged in Line 87–88 above it (depocenter B). A similar arcward bounding fault system is located in the northern survey region bordering depocenter D in Figure 12a. There is another large system of NNE-trending basement faults that cut across the central and northern forearc region dividing depocenters C and D. As interpreted, the southern NNE-trending fault system bends to a NE-trend north of Line 85, with fault offsets decreasing steadily to the north. The faults associated with this system are imaged on Line 30 as the high-angle normal faults separating the deeper basin to the south from the basement high to the north (Figure 6). The northern NNE-trending fault systems also bend to a NE-trend near 17.8°N toward Big Blue Seamount.

[64] After the late Eocene to early Oligocene rifting initiated the configuration of the forearc basin, sediment accumulated, often burying the basement structure. A late phase of extensional deformation occurred in the forearc during the end of Unit 5 deposition and throughout Unit 6. A GPS study shows that the forearc is currently under tension and that the Mariana arc-trench system is deforming nonrigidly [Kato *et al.*, 2003]. We suggest this deformation is accommodated by the late stage faulting that was and is occurring during deposition of Units 5 and 6. This most recent deformation uses the same NNE, NE, and NW fault trends as those of the late Eocene/early Oligocene rifting event. Figure 12b highlights seafloor-offset faults

imaged on seismic lines that can be traced in bathymetric data. Similar fault trends from both the Eo-Oligocene rifting and the Pliocene extensional deformation indicate that fault reactivation is occurring in the forearc. There is a higher density of normal faulting occurring in the region around 16.5°N. The seismic data also show that this extension affects the outer forearc basement and sediment more heavily than the inner forearc. The color-contoured isopach map in Figure 12b illustrates the thickness of Units 4 and 5, presumed to be from ~29 Ma to the present. These deposits accumulated in a single depocenter denoted by the blue shading.

[65] A study of fault patterns near 22°N, showed NE- and NW-trending faults in the forearc [Wessel *et al.*, 1994]. The authors concluded that these trends resulted from radial fracturing of the forearc due to increased arc curvature from Mariana Trough opening. The fact that the fault trends are similar at 22°N, 18°N, and 15°N argues that radial faulting may not be the cause of these modern fault patterns. Another possibility is that the fault trends observed today in the forearc are highlighting the Eo-Oligocene fault trends by reactivation. Seismic data support this idea with some of the largest seafloor offsets occurring above previously faulted basement blocks. Lines 30, 10–13, and 16–19 illustrate this trend (Figures 6, 9, and 10). This does not explain the increase in faulting in either the 16.5°N inner forearc region or more generally in the outer forearc.

4.5. Frontal Arc High Geometry and Forearc Subsidence

[66] It is a long outstanding question why the frontal arc high is so pronounced in the Mariana Forearc south of 17°N and why it appears absent north of 18°N. Since the remnants of the Eo-Oligocene arc make up this feature, it is unclear if the extent of the frontal arc high is related to the original structure of the Eo-Oligocene volcanic front or is controlled by other factors. Figure 13 shows the variation in frontal arc high and forearc basin geometry from north to south. The location of the NNE-trending basement faults active during Units 1 through 3 rifting are denoted by the black fault lines. Slip along this fault system controlled the amount of subsidence of the sedimentary basin relative to the frontal arc high. From this data, we propose a mechanism to explain the variation in frontal arc high bathymetry. These data suggest that the dramatic frontal arc high in the southern Mariana forearc is a result of uplift from a series of

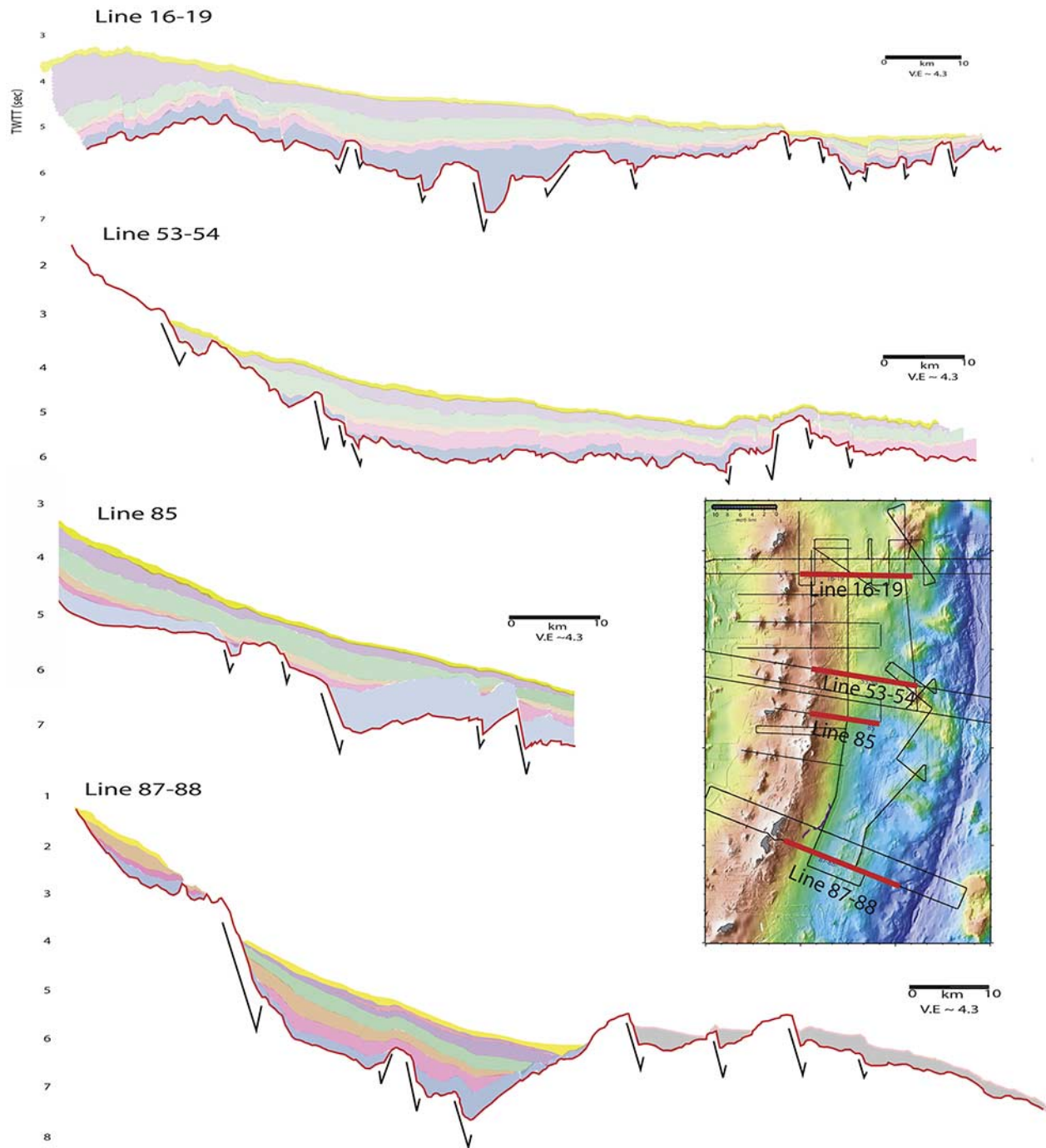


Figure 13. Schematic drawing of interpreted seismic lines across the forearc from north to south. The location of lines is shown on inset map in red. This figure highlights changes in forearc geometry. Tilted forearc slopes on Lines 85 and 87–88 indicate a trenchward tilting rotational event occurred in the southern forearc after deposition of Unit 5 sediment. Black arrows show the location of regional NNE-trending normal faults which created the deeply subsided southern forearc.

NNE-trending faults initiated during Eo-Oligocene rifting (Figure 13). South of 16.5°N , the footwall of the NNE-trending fault system and subsequently the frontal arc high of the Mariana forearc was

uplifted while the hanging wall subsided creating the deep forearc basin south of 16.5°N and the steep inner forearc slope imaged on Line 87–88. A system of NNE-trending faults does exist north of

17°N, but without comparable offset proximal to the frontal arc high. The absence of the frontal arc high in the 18°N region results in a nearly flat basement profile across the forearc to the trench slope break.

[67] Basin sediment slopes are also flat on all seismic profiles except the two lines in the southern region near 15°N (Line 85 and 87–88). The seismic data presented here show that the southern forearc has experienced dramatic rotation and trenchward tilting not seen elsewhere in the forearc. This rotation caused older horizontally deposited sediment to rotate to the current slopes imaged in the seismic data. The onlap of slope-bypassed Unit 6 sediment onto early Unit 6 deposits indicates that this rotation occurred very recently.

[68] One possible cause for this rotation is variation in the subducting slab geometry beneath the forearc. It has been observed in many convergent margins that the angle of the downgoing slab can vary along a subduction zone through time [Chiu *et al.*, 1991; Heuret and Lallemand, 2005]. In the Izu-Bonin-Mariana system, a slab tear between the Izu-Bonin and the Mariana segments of the convergent margin is well documented as the slab bends nearly vertically beneath the Mariana arc [Miller *et al.*, 2004, 2005]. A small change in slab dip beneath the forearc near ~16°N could explain the trenchward tilt of the forearc region imaged on the seismic data in the southern survey area. This shift in slab geometry would have begun during deposition of Unit 6.

[69] Models of subducting lithosphere in the Mariana margin from earthquake locations show a steeply dipping slab beneath the forearc from ~16°N to 20°N along the central portion of the arcuate margin [Chiu *et al.*, 1991]. North and south of this area, the margin curves westward giving way to the characteristic bow-shaped trench of the Mariana subduction zone. The 15°N region is a transitional boundary where deep earthquake activity ceases below 150 km. This is inferred to represent a change in slab dip beneath the forearc [Chiu *et al.*, 1991]. The tilting of the forearc imaged on the seismic data, a change in slab dip, and the deepening of the subducting slab by 2 km in the outer forearc near 15°N [Oakley *et al.*, 2008] argue that the subducting lithosphere may have recently deformed beneath the forearc most notably during Unit 6 deposition. This recent change in slab geometry would be affecting the inner forearc basin, up to 200 km away from the trench.

[70] Another possible explanation for the accelerated trenchward tilting of the 15°N region of the Marian forearc during Unit 6 deposition could be recent subduction of high bathymetry relief. It is noted in several convergent margins including many in the Pacific that subduction of aseismic ridges and volcanic edifices can greatly disturb the outer trench slope [Laurson *et al.*, 2002; Clift and Vannucchi, 2004; Bangs *et al.*, 2006]. Recent work on subducting slab geometry by Oakley *et al.* [2008] image several subducted seamounts beneath the Mariana outer forearc; however, there is little evidence for disturbance of the overlying plate above these bathymetric highs. The seismic data from this study did not show subducted relief in the tilted region of the forearc, though only two 2-D seismic lines cross the outer forearc. According to the proposed age for Unit 6, this trenchward tilting and possible high relief subduction would have to have occurred within the last 8 Ma.

5. Conclusions

[71] New seismic data collected over the Mariana forearc image six seismic stratigraphic sequences that are regionally correlatable across the forearc from 14°N to 18°N. Basement ridges and large-offset faults from early rifting have NE, NW, and NNE trends, and basement offset calculations show that this faulting accommodated ~4% extension. Sedimentary Units 1, 2, and 3 accumulated during forearc rifting after the formation of the forearc basement, likely during the late Eocene and early Oligocene. Unit 4 deposits correspond to a period of mild structural inversion in the Mariana forearc. Inversion may have been caused by seafloor spreading in the Parece-Vela Basin resulting in changes in forearc stresses. This is the first evidence for compression in the Mariana forearc. Units 5 and 6 accumulated during a later phase of extensional deformation that is ongoing today. We suggest that this extension results from the Mariana Trough backarc spreading that initiated ~8 Ma, is at least partly accommodated by reactivation of older basement faults, and is manifested in structures with the same NE, NW, and NNE trends. This late stage of deformation is most active in the inner forearc near 16.5°N and the outer forearc between 14.5°N and 18°N. A large normal growth fault system that initiated during early rifting is responsible for uplifting the frontal arc high in the southern forearc and creating a deep sedimentary basin between 14.5°N and 16.3°N. Along strike variation in forearc geometry may

indicate the location of a slab tear or recently subducted relief near 15°–16°N initiated during Unit 6.

Acknowledgments

[72] Careful and thoughtful reviews by David Scholl and Sean Gulick greatly improved this manuscript. Barrie Taylor, Andrew Goodliffe, and Adrienne Oakley provided MCS processing assistance that was essential to this project. We would also like to thank the crew of the R/V *Maurice Ewing* and the EW0202 cruise participants. This research was supported by NSF grant OCE-0001978 as part of the MARGINS Program. This is SOEST contribution 7563.

References

- Bangs, L. B., S. P. S. Gulick, and T. H. Shipley (2006), Seamount subduction erosion in the Nankai Trough and its potential impact on the seismogenic zone, *Geology*, *34*, 701–704, doi:10.1130/G22451.1.
- Bloomer, S. H. (1983), Distribution and origin of igneous rocks from the landward slopes of the Mariana Trench: Implications for its structure and evolution, *J. Geophys. Res.*, *88*, 7411–7428, doi:10.1029/JB088iB09p07411.
- Bloomer, S., B. Taylor, and C. J. Macleod (1995), Early arc volcanism and the ophiolite problem: A perspective from drilling the western Pacific, in *Active Margins and Marginal Basins of the Western Pacific*, *Geophys. Monogr. Ser.*, vol. 88, edited by B. Taylor and J. Natland, pp. 1–30, AGU, Washington, D. C.
- Chiu, J.-M., B. L. Isacks, and R. K. Cardwell (1991), 3-D configuration of subducted lithosphere in the western Pacific, *Geophys. J. Int.*, *106*, 99–111, doi:10.1111/j.1365-246X.1991.tb04604.x.
- Clift, P., and P. Vannucchi (2004), Controls on tectonic accretion versus erosion in subduction zones: Implications for the origin and recycling of the continental crust, *Rev. Geophys.*, *42*, RG2001, doi:10.1029/2003RG000127.
- Cooper, P. A., K. A. Dadey, A. Klaus, M. A. Lovell, P. A. Pezard, and B. Taylor (1992), Correlation of core and seismic stratigraphy by means of vertical seismic profiling, and downhole and physical properties measurements for the Leg 126 forearc Sites 787, 792, and 793, *Proc. Ocean Drill. Program Sci. Results*, *126*, 575–591.
- Cosca, M. A., R. J. Arculus, J. A. Pearce, and J. G. Mirchell (1998), ⁴⁰Ar/³⁹Ar and K-Ar age constraints for the inception and early evolution of the Izu-Bonin-Mariana arc system, *Isl. Arc*, *7*, 579–595, doi:10.1111/j.1440-1738.1998.00211.x.
- Dickinson, W., and D. R. Seely (1979), Structure and stratigraphy of forearc regions, *Am. Assoc. Pet. Geol. Bull.*, *63*, 2–31.
- Dobson, P. F., and R. O'Neil (1987), Stable isotope composition and water contents of boninite series volcanic rocks from Chichi-jima, Bonin Islands, Japan, *Earth Planet. Sci. Lett.*, *82*, 75–86, doi:10.1016/0012-821X(87)90108-7.
- Engdahl, E. R., R. D. van der Hilst, and R. P. Buland (1998), Global teleseismic earthquake relocation with improved travel times and procedures for depth determination, *Bull. Seismol. Soc. Am.*, *88*, 722–743.
- Forsyth, D. W., and S. Uyeda (1975), On the relative importance of the driving forces of plate motion, *Geophys. J.*, *43*, 163–200, doi:10.1111/j.1365-246X.1975.tb00631.x.
- Froidevaux, C., S. Uyeda, and M. Uyeshima (1988), Island arc tectonics, *Tectonophysics*, *148*, 1–9, doi:10.1016/0040-1951(88)90156-4.
- Fryer, P. (1992a), Mud volcanoes of the Marianas, *Sci. Am.*, *266*, 46–52.
- Fryer, P. (1992b), A synthesis of Leg 125 drilling of serpentine seamounts on the Mariana and Izu-Bonin forearcs, *Proc. Ocean Drill. Program Sci. Results*, *125*, 593–614.
- Fryer, P., C. G. Wheat, and M. J. Mottl (1999), Mariana blueschist mud volcanism: Implications for conditions within the subduction zone, *Geology*, *27*, 103–106, doi:10.1130/0091-7613(1999)027<0103:MBMVIF>2.3.CO;2.
- Heuret, A., and S. Lallemand (2005), Plate motion, slab dynamics and back-arc deformation, *Phys. Earth Planet. Inter.*, *149*, 31–51, doi:10.1016/j.pepi.2004.08.022.
- Hilton, D. R., J. S. Pallister, and R. M. Pua (2005), Introduction to the special issue on the 2003 eruption of Anatahan Volcano, Commonwealth of the Northern Mariana Islands (CNMI), *J. Volcanol. Geotherm. Res.*, *146*, 1–7, doi:10.1016/j.jvolgeores.2005.01.015.
- Huang, W.-C., and E. Okal (1998), Centroid-moment-tensor solutions for deep earthquakes predating the digital era: Discussion and inferences, *Phys. Earth Planet. Inter.*, *106*, 191–218, doi:10.1016/S0031-9201(97)00111-8.
- Hussong, D. M. (1981), Underway geophysics-Leg 60 and related surveys, *Initial Rep. Deep Sea Drill. Proj.*, *60*, 71–73.
- Hussong, D. M., and P. Fryer (1981), Structure and tectonics of the Mariana Arc and Forarc: Drillsite selection surveys, *Initial Rep. Deep Sea Drill. Proj.*, *60*, 33–44.
- Hussong, D. M., and P. Fryer (1983), Back-arc seamounts and the SeaMARC II seafloor mapping system, *Eos Trans. AGU*, *64*, 627–632.
- Hussong, D. M., and J. B. Sinton (1983), Seismicity associated with back arc crustal spreading in the central Mariana Trough, in *The Tectonic and Geologic Evolution of Southeast Asian Seas and Islands, Part 2*, *Geophys. Monogr. Ser.*, vol. 27, edited by D. E. Hayes, pp. 217–235, AGU, Washington, D. C.
- Hussong, D. M., and S. Uyeda (1981), Tectonic processes and the history of the Mariana arc: A synthesis of the results of Deep Sea Drilling Project Leg 60, *Initial Rep. Deep Sea Drill. Proj.*, *60*, 909–929.
- Hyndman, R. D., and S. M. Peacock (2003), Serpentinization of the forearc mantle, *Earth Planet. Sci. Lett.*, *212*, 417–432, doi:10.1016/S0012-821X(03)00263-2.
- Isacks, B. L., and M. Barazangi (1977), Geometry of Benioff Zones: Lateral segmentation and downwards bending of the subducted lithosphere, in *Island Arcs, Deep Sea Trenches, and Back-Arc Basins, Maurice Ewing Ser.*, vol. 1, edited by M. Talwani and W. C. Pitman, pp. 99–114, AGU, Washington, D.C.
- Ishizuka, O., et al. (2006), Early stages in the evolution of Izu-Bonin arc volcanism: New age, chemical, and isotopic constraints, *Earth Planet. Sci. Lett.*, *250*, 385–401, doi:10.1016/j.epsl.2006.08.007.
- Karig, D. E. (1971a), Origin and development of marginal basins in the western Pacific, *J. Geophys. Res.*, *76*, 2542–2561, doi:10.1029/JB076i011p02542.
- Karig, D. E. (1971b), Structural history of the Mariana island arc system, *Geol. Soc. Am. Bull.*, *82*, 323–344, doi:10.1130/0016-7606(1971)82[323:SHOTMI]2.0.CO;2.
- Karig, D. E., and B. Ranken (1983), Marine geology of the forearc region, southern Mariana island arc, in *The Tectonic and Geologic Evolution of the Southeast Asian Seas and Islands: Part 2, Geophys. Monogr. Ser.*, vol. 27, edited by D. E. Hayes, pp. 266–280, AGU, Washington, D. C.

- Kato, T., J. Beavan, T. Matsushima, Y. Kotake, J. Camacho, and S. Nakao (2003), Geodetic evidence of back-arc spreading in the Mariana Trough, *Geophys. Res. Lett.*, *30*(12), 1625, doi:10.1029/2002GL016757.
- Katsumata, M., and L. Sykes (1969), Seismicity and tectonics of the western Pacific: Izu-Mariana-Caroline and Ryukyu-Taiwan regions, *J. Geophys. Res.*, *74*, 5923–5948, doi:10.1029/JB074i025p05923.
- Kitada, K., N. Seama, T. Yamazaki, Y. Nogi, and K. Suyehiro (2006), Distinct regional differences in crustal thickness along the axis of the Mariana Trough, inferred from gravity anomalies, *Geochem. Geophys. Geosyst.*, *7*, Q04011, doi:10.1029/2005GC001119.
- Koppers, A. A. P., and H. Staudigel (2005), Asynchronous bend in Pacific Seamount Trails: A case for extensional volcanism?, *Science*, *307*, 904–907, doi:10.1126/science.1107260.
- LaTraille, S. L., and D. M. Hussong (1980), Crustal structure across the Mariana island arc, in *The Tectonic and Geologic Evolution of Southeast Asian Seas and Islands: Part 1, Geophys. Monogr. Ser.*, vol. 23, edited by D. E. Hayes, pp. 209–221, AGU, Washington, D. C.
- Laursen, J., D. W. Scholl, and R. von Huene (2002), Neotectonic deformation of the central Chile margin: Deepwater forearc basin formation in response to hot spot ridge and seamount subduction, *Tectonics*, *21*(5), 1038, doi:10.1029/2001TC901023.
- Letouzey, J. (1990), Fault reactivation, inversion and fold-thrust belt, in *Petroleum and Tectonics in Mobile Belts*, edited by J. Letouzey, pp. 101–128, Technip, Paris.
- Martinez, F., P. Fryer, N. A. Baker, and T. Yamazaki (1995), Evolution of backarc rifting: Mariana Trough, 20°–24°N, *J. Geophys. Res.*, *100*, 3807–3827, doi:10.1029/94JB02466.
- Martinez, F., P. Fryer, and N. Becker (2000), Geophysical characteristics of the southern Mariana Trough, 11°50′N–13°40′N, *J. Geophys. Res.*, *105*, 16,591–16,608, doi:10.1029/2000JB900117.
- Miller, M. S., B. L. N. Kennett, and G. S. Lister (2004), Imaging changes in morphology, geometry, and physical properties of the subducting Pacific plate along the Izu-Bonin-Mariana arc, *Earth Planet. Sci. Lett.*, *224*, 363–370, doi:10.1016/j.epsl.2004.05.018.
- Miller, M. S., A. Gorbato, and B. L. N. Kennett (2005), Heterogeneity within the subducting Pacific slab beneath the Izu-Bonin-Mariana arc: Evidence from tomography using 3D ray tracing inversion techniques, *Earth Planet. Sci. Lett.*, *235*, 331–342, doi:10.1016/j.epsl.2005.04.007.
- Mrozowski, C. L., and D. E. Hayes (1979), The evolution of the Parece Vela Basin, eastern Philippine Sea, *Earth Planet. Sci. Lett.*, *46*, 49–67, doi:10.1016/0012-821X(79)90065-7.
- Mrozowski, C. L., and D. E. Hayes (1980), A seismic reflection study of faulting in the Mariana fore arc, in *The Tectonic and Geologic Evolution of Southeast Asian Seas and Islands: Part 1, Geophys. Monogr. Ser.*, vol. 23, edited by D. E. Hayes, pp. 223–234, AGU, Washington, D. C.
- Mrozowski, C. L., D. E. Hayes, and B. Taylor (1981), Multi-channel seismic reflection surveys of Leg 60 sites, Deep Sea Drilling Project, *Initial Rep. Deep Sea Drill. Proj.*, *60*, 57–69.
- Nakanishi, M., K. Tamaki, and K. Kobayashi (1992), A new Mesozoic isochron chart of the northwestern Pacific Ocean: Paleomagnetic and tectonic implications, *Geophys. Res. Lett.*, *19*, 693–696, doi:10.1029/92GL00022.
- Oakley, A. J., B. Taylor, E. L. Chapp, and G. Moore (2006), Imaging the subducting Pacific plate beneath the Mariana Forearc, *Eos Trans. AGU*, *87*(52), Fall Meet. Suppl., Abstract T53A–1403.
- Oakley, A. J., B. Taylor, and G. F. Moore (2008), Pacific Plate subduction beneath the central Mariana and Izu-Bonin fore-arc: New insights from an old margin, *Geochem. Geophys. Geosyst.*, *9*, Q06003, doi:10.1029/2007GC001820.
- Okino, K., S. Kasuga, and Y. Ohara (1998), A new scenario of the Parece Vela Basin genesis, *Mar. Geophys. Res.*, *20*, 21–40, doi:10.1023/A:1004377422118.
- Scott, R., and L. Kroenke (1983), Evolution of back arc spreading and arc volcanism in the Philippine Sea: Interpretation of Leg 59 DSDP results, in *The Tectonic and Geologic Evolution of Southeast Asian Seas and Islands: Part 2, Geophys. Monogr. Ser.*, vol. 27, edited by D. Hayes, pp. 283–291, AGU, Washington, D. C.
- Scott, R. B., L. W. Kroenke, G. Zakariadze, and A. Sharaskin (1980), Evolution of the South Philippine Sea: Deep Sea Drilling Project Leg 59 results, *Initial Rep. Deep Sea Drill. Proj.*, *59*, 803–815.
- Sdrolias, M., W. R. Roest, and R. D. Muller (2004), An expression of Philippine Sea Plate rotation: The Parece Vela and Shikoku Basins, *Tectonophysics*, *394*, 69–86, doi:10.1016/j.tecto.2004.07.061.
- Seama, N., and T. Fujiwara (1993), Geomagnetic anomalies in the Mariana Trough, 18°N, in *Preliminary Report of the Hakuho-Maru Cruise KH92-1*, edited by J. Segawa, pp. 70–73, Ocean Res. Inst., Univ. of Tokyo, Tokyo.
- Sharp, W., and D. Clague (2006), 50-Ma initiation of Hawaiian-Emperor Bend records major change in Pacific plate motion, *Science*, *313*, 1281–1284, doi:10.1126/science.1128489.
- Shipboard Scientific Party (1978a), Site 447: East side of the West Philippine Basin, *Initial Rep. Deep Sea Drill. Proj.*, *60*, 1–110.
- Shipboard Scientific Party (1978b), Site 448: Palau-Kyushu Ridge, *Initial Rep. Deep Sea Drill. Proj.*, *60*, 111–320.
- Shipboard Scientific Party (1978c), Site 458: Mariana Fore-Arc, *Initial Rep. Deep Sea Drill. Proj.*, *60*, 263–308.
- Shipboard Scientific Party (1978d), Site 459: Mariana Fore-Arc, *Initial Rep. Deep Sea Drill. Proj.*, *60*, 309–369.
- Shipboard Scientific Party (1990a), Site 787, *Proc. Ocean Drill Program Initial Rep.*, *126*, 63–96.
- Shipboard Scientific Party (1990b), Site 792, *Proc. Ocean Drill Program Initial Rep.*, *126*, 221–314.
- Shipboard Scientific Party (1990c), Site 793, *Proc. Ocean Drill Program Initial Rep.*, *126*, 315–403.
- Stern, R. J., and N. C. Smoot (1998), A bathymetric overview of the Mariana forearc, *Isl. Arc*, *7*, 525–540, doi:10.1111/j.1440-1738.1998.00208.x.
- Stern, R., M. J. Fouch, and S. L. Klemperer (2003), An overview of the Izu-Bonin-Mariana Subduction Factory, in *Inside the Subduction Factory, Geophys. Monogr. Ser.*, vol. 138, edited by J. Eiler and M. Hirschmann, pp. 175–222, AGU, Washington, D. C.
- Tarduno, J. A. (2007), On the motion of Hawaii and other mantle plumes, *Chem. Geol.*, *241*, 234–247, doi:10.1016/j.chemgeo.2007.01.021.
- Taylor, B. (1992), Rifting and the volcanic-tectonic evolution of the Izu-Bonin-Mariana arc, *Proc. Ocean Drill. Program Sci. Results*, *126*, 627–651.
- Taylor, B., and A. Goodliffe (2004), The West Philippine Basin and the initiation of subduction, revisited, *Geophys. Res. Lett.*, *31*, L12602, doi:10.1029/2004GL020136.
- Taylor, B., G. Moore, A. Klaus, M. Systrom, P. Cooper, and M. MacKay (1990), Multichannel seismic survey of the central Izu-Bonin Arc, *Proc. Ocean Drill. Program Initial Rep.*, *126*, 51–60.

- Terrinha, P., C. Ribeiro, J. C. Kullberg, C. Lopes, R. Rocha, and A. Ribeiro (2002), Compressive episodes and faunal isolation during rifting, southwest Iberia, *J. Geol.*, *110*, 101–113, doi:10.1086/324206.
- Uyeda, S. (1982), Subduction zones: An introduction to comparative subductology, *Tectonophysics*, *81*, 133–159, doi:10.1016/0040-1951(82)90126-3.
- Wessel, J. K., P. Fryer, P. Wessel, and B. Taylor (1994), Extension in the northern Mariana inner forearc, *J. Geophys. Res.*, *99*, 15,181–15,203, doi:10.1029/94JB00692.
- Whittaker, J. M., R. D. Muller, G. Leitchenkov, H. Stagg, M. Sdrolias, C. Gaina, and A. Goncharov (2007), Major Australian-Antarctic plate reorganization at Hawaiian-Emperor Bend time, *Science*, *318*, 83–86, doi:10.1126/science.1143769.